"The **more** opportunities there are to get **students involved**, the more you will **encourage** previously unreached and **unrepresented groups** to join the Earth and Space science community."

**Ryan Haupt**
Research Fellow,
Smithsonian Museum
of Natural History
2015 Student Travel
Grant Recipient

**Support the next generation of Earth and space scientists.**
**Donate to the Austin Student Travel Grant Challenge.**

AGU100 ADVANCING EARTH AND SPACE SCIENCE

**agu.org/austin | #AGU100**

Water Resources Research

RESEARCH ARTICLE
10.1029/2019WR024819

# Analysis of Flow Resistance Equations in Gravel-Bed Rivers With Intermittent Regimes: Calabrian *fiumare* Data Set

**G. Mendicino**[1] and **F. Colosimo**[2]

[1]Department of Environmental and Chemical Engineering, University of Calabria, Rende, Italy, [2]Freelance Environmental Engineer, Rende, Italy

**Key Points:**
- New flow resistance equations in gravel-bed rivers
- Effects induced by Froude number and sediment mobility parameter
- Flow resistance in large-scale roughness.

**Supporting Information:**
- Supporting Information S1
- Table S1
- Figure S1
- Figure S2
- Figure S3
- Figure S4
- Figure S5
- Figure S6
- Figure S7
- Figure S8
- Figure S9
- Figure S10
- Figure S11

**Correspondence to:**
G. Mendicino,
giuseppe.mendicino@unical.it

**Citation:**
Mendicino, G., & Colosimo, F. (2019). Analysis of flow resistance equations in gravel-bed rivers with intermittent regimes: Calabrian *fiumare* data set. *Water Resources Research*, *55*. https://doi.org/10.1029/2019WR024819

Received 1 FEB 2019
Accepted 6 AUG 2019
Accepted article online 10 AUG 2019



**Abstract** This study addresses the evaluation of flow resistance in natural gravel-bed rivers. Through a new data set collected on 136 reaches of 78 gravel-bed rivers (Calabrian *fiumare*) in southern Italy, different conventional flow resistance equations to predict mean flow velocity in gravel-bed rivers were tested in their original form. These equations have shown considerable disagreement with observed data, especially in river reaches characterized by high bed load conditions and for the domains of intermediate- and large-scale roughness. This disagreement produced in almost all the cases an underestimation of the flow resistance, which can be corrected by introducing the Froude number and a particular form of the Shields sediment mobility parameter into the Manning, Chezy, and Darcy-Weisbach equations. Through analyses carried out both on the whole data set and on its subsets, we propose a semiempirical approach with which, on the one hand, the tractive forces exerted by the flow on the bed are taken into account by considering the ratio between the sediment mobility parameter and its critical value, and on the other hand, water surface distortions are evaluated using the Froude number. This approach has been further validated using a literature-based data set showing, even in this case, excellent performances. Finally, the literature-based data set allowed us to improve the performances of the proposed approach in the field of large-scale roughness. Efficiency tests indicate that the new equations can better reproduce the flow velocity in river reach where conventional flow resistance equations are not able to explain the entire dissipative process.

## 1. Introduction

Flow velocity estimation in natural gravel-bed rivers, despite many scientific contributions to date in the literature, is still a problem of extreme interest due to the many technical and scientific implications (flow discharge, river engineering, risk assessment, numerical modeling validation, etc.) that have not yet been completely solved. The research carried out so far while providing valid flow resistance equations shows nonnegligible limitations due to the simplifications present in the estimation models used. Regarding these limitations, simplified conditions such as steady flow, one-dimensional and uniform flow, completely turbulent regime, very wide and geometrically defined cross section with no vegetation, flat gravel-bed, and absence of bed load transport seem to be not enough distinct to establish with precision, for the different situations taking place in nature, absolute threshold values able to separate one condition from another.

The increasing availability of measured data has shown that in the case of low-gradient rivers mainly characterized by sandy and small gravel-bed channels, flow resistance equations can provide acceptable performances (Yen, 1992), but in the case of high-gradient channels with gravel and coarse bed materials, flow resistance estimation becomes more complicated and less efficient (Wohl, 2000). Furthermore, different dissipative mechanisms are observed according to the values assumed by the relative submergence of flow (Bathurst et al., 1981), expressed by the ratio between the hydraulic radius $R$ or the mean flow depth $y_m$ and the characteristic diameter $d_{\Phi\ (50\ or\ 84)}$ (which represents a nominal diameter $\Phi$ for which 50 or 84 percent of the sediment mixture by weight is smaller). For high relative submergence values (greater than 10) the main flow resistance sources are due to the form drag on individual bed particles and viscous friction on their surfaces (skin friction), also taking into account any large-scale bed-form characteristic. For low relative submergence values (close to 1) form drag together with the turbulent wakes of large roughness elements seems to be relatively greater, and further losses can be observed if flow is locally supercritical and

wave drag occurs on any elements protruding above the water surface (Ferguson, 2007; Nitsche et al., 2012; Rickenmann & Recking, 2011). Another aspect strongly influencing flow resistance is represented by the shear stress exerted by the flow on the bed (bed load transport). Many researchers have widely demonstrated that the bed load increases the flow resistance (Baiamonte & Ferro, 1997; Bergeron & Carbonneau, 1999; Campbell et al., 2005; Carbonneau & Bergeron, 2000; Ferro, 2018b; Gao & Abrahams, 2004; Recking et al., 2008, Smart & Jaeggi, 1983; Song et al., 1995), because it extracts momentum from the flow, which causes a reduction in flow velocity and an increase in the apparent roughness length in proportions that are related to the thickness of the moving sediment layer. Specifically, Recking et al. (2008), studying the feedback between bed load transport and flow resistance in gravel and cobble bed rivers, indicated that this tractive force, responsible for bed load, cannot be estimated only through a resistance coefficient representative of a constant bed roughness, especially for very high bed load rates.

As a consequence of the dissipative phenomena just described, flow resistance equations similar to those suggested by Strickler (1923), Keulegan (1938), Limerinos (1970), Hey (1979), Smart and Jaeggi (1983), Jarrett (1984), Bathurst (1985, 2002), Ferguson (2007), Rickenmann and Recking (2011), and many more can provide nonnegligible overestimates of mean flow velocity values especially when, to the pattern and arrangement of the roughness elements in the channel, a flow resistance increase is added because of bed load transport.

The same equations may show further errors when dissipative phenomena occur due to changes in flow regime (supercritical, subcritical, or critical) and free-surface instabilities and hydraulic jumps, especially when low values of relative submergence take place. These energy losses vary significantly according to the Froude number, which therefore can be considered a useful indicator of flow dissipative effects.

Different studies highlighted the benefits produced by the Froude number in the flow resistance estimation (Afzalimehr & Anctil, 1998; Bathurst, 1982; Bathurst et al., 1981; Camacho & Yen, 1991; Chow, 1959; Colosimo et al., 1988; Colosimo et al., 1991; Dìaz, 2005; Di Stefano et al., 2018; Ferro, 2003; Ferro, 2017; Ferro & Porto, 2018; Graf et al., 1983; Iwagaki, 1954; Lawrence, 1997; Rosso et al., 1990; Rouse et al., 1963; Ugarte Soto & Madrid-Aris, 1994; Wang & Dawdy, 2014; Zhang et al., 2010).

In order to evaluate all the dissipative phenomena described so far, Colosimo et al. (1988, 1991) proposed a flow resistance relationship taking into account the influence of both the Froude number and the ratio between a particular form of the Shields sediment mobility parameter (1936), suggested by Yalin $Y$ (1972), and its critical value $Y_{cr}$, proposed by Ackers and White (1973). Following the same idea of Colosimo et al. (1988), Afzalimehr and Anctil (1998) using a broad field data set of 280 gravel-bed rivers located in different parts of the world confirmed the benefits of introducing the Froude number and the Shields sediment mobility parameter in a semilogarithmic flow resistance equation. Recently, this result has been also confirmed by Ferro and Porto (2018) who, investigating the possibility of applying the self-similarity hypothesis to flow-resistance laws, have demonstrated the dependence of flow resistance on the Reynolds, Froude, and Shields (1936) numbers.

Therefore, in this paper, through the use of new field topographic, granulometric, and hydraulic measurements carried out on approximately 1,000 cross sections of 136 reaches of 78 gravel-bed rivers (Calabrian *fiumare*) in Southern Italy during the period 2014–2016, (1) the performance of different conventional flow resistance equations is evaluated, (2) new flow resistance equations considering an overall resistance coefficient composed by two terms: the former concerning the grain resistance term (friction coefficient) and the latter incorporating the interactions among channel hydraulics, riverbed configuration, and bed load transport dynamics are proposed. Specifically, in the latter term according to the scale roughness considered (as a function of the relative submergence), the effects due to free-surface instabilities, hydraulic jumps, and other losses related to flow regime changing were taken into account by the Froude number, while all the energy losses due to the bed load transport were evaluated by the $Y/Y_{cr}$ ratio. Through calibration procedures carried out on a subset of the whole Calabrian data set, the term including both the Froude number and the $Y/Y_{cr}$ ratio has been achieved. Then (3), the new and the conventional equations have been validated on another subset of the Calabrian data set characterized by very high bed load rates. Following (4), a literature-based data set composed of about 2,000 field data from miscellaneous rivers was used, on the one hand, to prove the suitability of the new equations, and on the other, to improve the performances of the same in the field of large-scale roughness.

In section 2, different conventional flow resistance equations are presented for evaluation. In the third section, the Calabrian data set is described, as well as a literature-based data set. Next, in the fourth section, the conventional flow resistance equations are considered to test the Calabrian data set (initially as a whole and then subdivided for with and without bed load and for relative submergence classes). Section 5 focuses on the effects produced by the Froude number and the $Y/Y_{cr}$ ratio on the estimate of flow resistance. Finally, in section 6, the results obtained are discussed.

## 2. Flow Resistance Equations

Flow resistance estimates start from the parameterization of quantities mainly based on the flow velocity $U$ (L/T); mean flow depth $y_m$ (L); energy slope of the water profile, equal to the friction slope in uniform steady flow $S_f$ (-); and bottom shear stress $\tau$ ($ML^{-1}/T^2$), according to a functional scheme such as this

$$U \propto R^{a_1} S_f^{a_2} \tag{1}$$

where $R$ (L) is the hydraulic radius, equivalent to the mean flow depth $y_m$ (L) in the case of a very wide section (width/depth > 20), and $a_1$ and $a_2$ are two empirical exponents. According to equation (1), the most well-known equations defining the link between flow resistance and the parameters just mentioned are those of Manning, Chezy, and Darcy-Weisbach, which can be equated to one another as follows:

$$U = \frac{S_f^{1/2} R^{2/3}}{n} = C\sqrt{RS_f} = \sqrt{\frac{8gRS_f}{f}} \tag{2}$$

where $n$ is equal to the Manning coefficient ($T/L^{1/3}$), $C$ is equal to the Chezy coefficient ($L^{1/2}/T$), $f$ is equal to the Darcy-Weisbach friction factor (dimensionless), and $g$ ($L/T^2$) is equal to the acceleration due to gravity.

Many methods for evaluating the $n$ and $C$ coefficients and the friction factor $f$ exist (Namaee et al., 2017; Powell, 2014; Rickenmann & Recking, 2011; Yen, 1992; Yochum et al., 2012). In this study, we analyzed different types of formulations: those empirically based on regression (power-law equations), those semianalytically based on boundary-layer theory (semilogarithmic equations), and combined formulations based on the definition of the variable-power resistance equation (VPE).

More specifically, different equations for the estimation of the coefficient $n$ were analyzed. Starting from the simplest, based on a power law concerning the characteristic diameter $d_\Phi$ of the material constituting the bottom of the river reach, we considered the equations proposed by Strickler (1923):

$$n = \frac{1}{21.1} d_{50}^{1/6} \tag{3}$$

where $d_{50}$ is equal to the nominal diameter larger than 50% by weight of the sediment mixture. Ferguson (2010) and Rickenmann and Recking (2011) noted that the Manning-Strickler equations, except in special cases, tend to underestimate flow resistance due to the mode by which they were obtained. Then, the equation suggested by Limerinos (1970)

$$\frac{n}{R^{1/6}} = \frac{0.1129}{1.16 + 2.0\log\left(\frac{R}{d_{84}}\right)} \tag{4}$$

reveals the effects caused by introducing only the relative submergence $R/d_{84}$ (with $d_{84}$ equal to the nominal diameter larger than 84% by weight of the sediment mixture). Alternatively, $n$ can be determined by following the purely empirical approach proposed by Jarrett (1984):

$$n = 0.32\, S_f^{0.38}\, R^{-0.16} \tag{5}$$

Next, by considering the law of the wall initially developed by Keulegan (1938) to estimate the dimensionless friction factor $f$ and integrating the well-known equation of Prandtl-von Karman-Nikuradse for the logarithmic mean flow velocity profile, a set of logarithmic equations was also considered in a form such as this

$$\sqrt{\frac{8}{f}} = \frac{U}{u^*} = 6.25 + \frac{1}{\boldsymbol{k}} log\left(\frac{R}{k_s}\right) \tag{6}$$

where $u^* = (g\,R\,S_f)^{0.5}$ represents the shear velocity (L/T), $k_s$ (L) is the bed roughness, and $\boldsymbol{k}$ indicates the von Karman constant, equal to 0.4. In our study, the roughness $k_s$, according to Hey (1979), was assumed to be equal to 3.5 $d_{84}$.

The friction factor $f$ has been further evaluated through different approaches, from the semilogarithmic method proposed by Bathurst (1985):

$$\sqrt{\frac{8}{f}} = 5.62\ log\left(\frac{R}{d_{84}}\right) + 4.00 \tag{7}$$

to others, such as Smart and Jaeggi (1983)

$$\sqrt{\frac{8}{f}} = 5.75\left[1 - exp\left(-0.05\,\frac{R}{d_{90}}\frac{1}{\sqrt{S_f}}\right)\right] log\left(8.2\,\frac{R}{d_{90}}\right) \tag{8}$$

with $d_{90}$ equal to the nominal diameter larger than 90% by weight of the sediment mixture.

Among the equations based on the Chezy coefficient estimation, we decided to consider the approach presented by Chow (1959), which modified the Keulegan equation (6) by incorporating the results obtained by Iwagaki (1954):

$$\frac{U}{u^*} = \frac{C}{\sqrt{g}} = A_r + 5.75\log\left(\frac{R}{k_s}\right) \tag{9}$$

where $C$ is the Chezy coefficient, expressed for riverbeds in rough flow conditions according to the following equation:

$$C = 5.75\sqrt{g}\left[\frac{A_r}{5.75} + \log\left[\frac{R}{k_s}\right]\right] = 18\,\log\left[10^{\frac{A_r}{5.75}}\frac{R}{k_s}\right] \tag{10}$$

where $A_r$ represents the Iwagaki coefficient, which is valid for $Fr$ values between 0.2 and 8.0 and is equal to

$$A_r = -27.058\log(Fr + 9) + 34.289 \tag{11}$$

The choice of this equation lies in the fact that it does not only take into account the grain resistance but, through the presence of the Froude number also considers the hydraulic effects of the flow and the free-surface instabilities.

Many of the above equations can be applied only for small-scale roughness conditions, that is, according to Bathurst et al. (1981), when the hydraulic radius $R$ or the mean flow depth $y_m$ is much higher than the characteristic diameter $d_{84}$. When $R$ or $y_m$ is of the same order of magnitude as the bed roughness height, then large-scale roughness conditions occur in a river reach. For these conditions, several authors, including Ferguson (2007), Comiti et al. (2007), and Rickenmann and Recking (2011), have demonstrated that due to irregularities in the bed topography and water surface, it is difficult to carry out reliable measurements of the representative flow depth to be used in the common resistance equations. Therefore, the same authors have suggested the use of dimensionless variables to represent the hydraulic characteristics of the flow in a form such as this

$$U^{**} = k^{**}\,q^{**}\ with\ U^{**} = \frac{U}{\sqrt{g\,S_f\,d_{84}}} \quad \text{and} \quad q^{**} = \frac{q}{\sqrt{g\,S_f\,d_{84}}} \tag{12}$$

where $q$ is the unit discharge and $k^{**}$ is an empirical coefficient.

This approach derives from studies initially carried out by Ferguson (2007) on flow resistance equations in steep streams with beds dominated by gravel, cobbles, and boulders, which led to the definition of the variable-power resistance equation which is the product of a combination of the Manning-Strickler approximation of the logarithmic friction law for deep flow, where $R/d_{84}$ is very large, and the roughness-layer formulations for shallow flow (Lawrence, 1997; Nikora, et al., 2001), where $R/d_{84}$ is very small. In our study, we analyzed two VPE-based equations. The first equation was provided by Ferguson (2007) and assumes the Darcy-Weisbach friction factor $f$ to be the sum of two components while taking into account the bed form and skin friction effects, thus providing a single resistance equation applicable to both shallow and deep flows over coarse riverbeds:

$$\sqrt{\frac{8}{f}} = \frac{U}{u^*} = \frac{b_1 b_2 \left(\frac{R}{d_{84}}\right)}{\sqrt{{b_1}^2 + {b_2}^2 \left(\frac{R}{d_{84}}\right)^{1.67}}} \tag{13}$$

with $b_1 = 6.5$ and $b_2 = 2.5$ (Ferguson, 2007), which is suitable for all relative submergence values $R/d_{84}$ . The second equation was proposed by Rickenmann and Recking (2011), who, using a data set of 2890 field measurements, suggested a modified Ferguson's equation as follows:

$$\sqrt{\frac{8}{f}} = \frac{U}{u^*} = \frac{4.416 \left(\frac{R}{d_{84}}\right)^{1.904}}{\left[1 + \left(\frac{R}{1.283\ d_{84}}\right)^{1.618}\right]^{1.083}} \tag{14}$$

## 3. The Data Set

Field measurements were collected in river reaches belonging to the Italian Apennine mountain chain. These rivers are included in the well-known category of *fiumare*, which show typical high gradients, short lengths, and distributed gravel-bed material (Sabato & Tropeano, 2004). This kind of river shows an intermittent rather than continuous sediment-transport process, and the flow is characterized by an irregular hydrometric regime.

Specifically, starting from a total of approximately 1,000 cross sections, new data were collected during the period 2014–2016 along 136 straight reaches of 78 gravel-bed rivers in Calabria (southern Italy; Figure 1). These measurements were performed monthly on each river reach, producing an initial database of approximately 1,000 measurements of flow velocity and related topographic, granulometric, and hydraulic parameters. The 136 gravel-bed reaches were chosen in such a way that the measurements were characterized by steady, one-dimensional, uniform flow; as much as possible, the reaches were straight and free of macroscopic disturbances.

For each reach, the bed slope was defined by measuring the water level (in an undisturbed zone of the cross section) between two cross sections located at the beginning and the end of the reach. The cross section located in the middle of the reach was hypothesized to be representative of the whole reach and was surveyed for measurements of flow velocity. Discharge and flow velocity measurements were obtained using a three-dimensional flow tracker based on the proven Acoustic Doppler velocimeter (ADV) technology. The sensor, working to 500 kHz, allows reliable measurements starting from flow depths greater than 25 mm, with a maximum tolerance of $\pm$8 mm. The discharge measurements were carried out according to the following steps: (1) A graduated tag line was laid across the river reach; (2) with the ADV probe maintained perpendicular to the tag line, a number of spaced vertical lines, with intervals ranging between 0.50 and 1.00 m, were defined based on the width of the river reach; (3) for each vertical, water depth and flow velocity were recorded at a given depth (at 0.5 $y$); (4) the single flow velocity value was multiplied by the portion of the cross-sectional area related to the corresponding vertical of measurement to determine the single discharge $q_i$; and finally, the total discharge Q was determined by integrating all the $q_i$ values achieved previously. On the same reach, granulometric characteristics were determined through direct sampling and subsequent definition of the grain-size distribution curve, from which the grain sizes $d_{90}$, $d_{84}$, $d_{50}$, and $d_{16}$ were extracted. In particular, following empirical study (Bathurst, 2002; Hey, 1979; Limerinos, 1970;

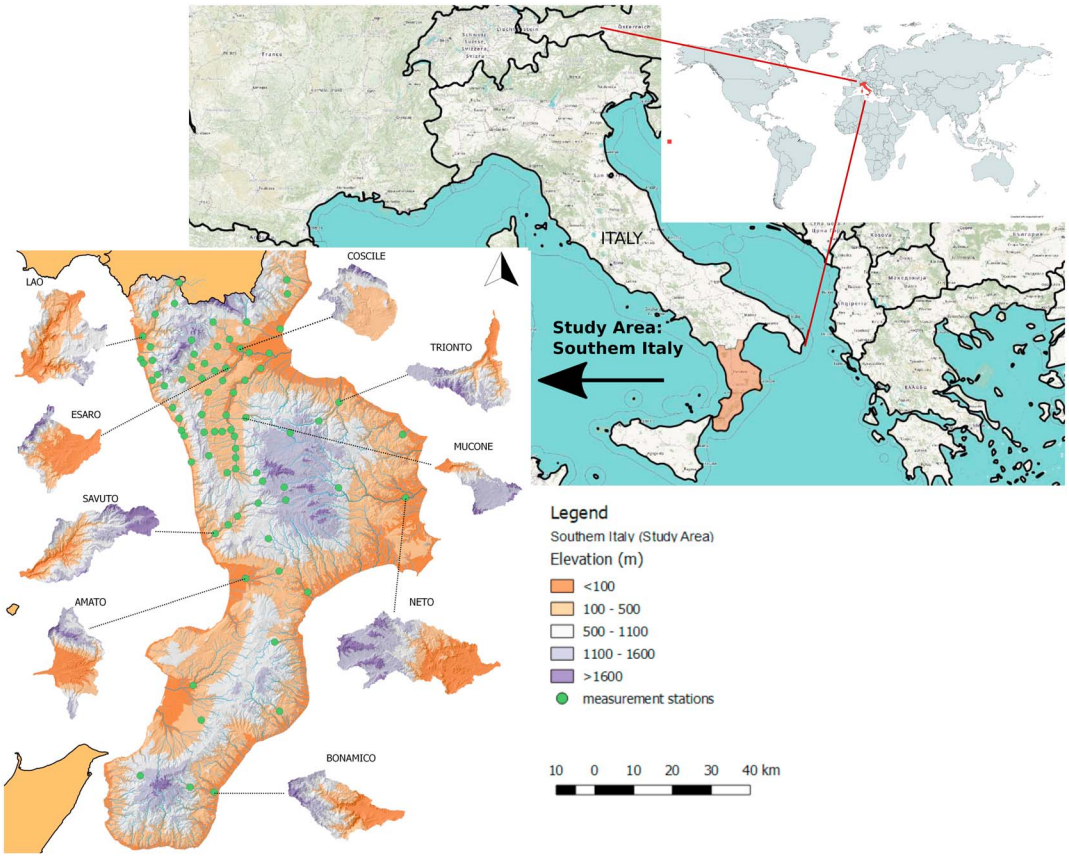


**Figure 1.** Geolocation of the river sections considered for the data set (southern Italian region of Calabria).

and many more) and theoretical analysis (MacKenzie et al., 2018; Wiberg & Smith, 1991), the 84-percentile size of the bed material was assumed as the dominant sediment length scale for flow over nonuniform bed material and then representative of the roughness height within the flow resistance equations.

From the measured values of the flow discharge $Q$ ($L^3/T$), flow cross-sectional area $A$ ($L^2$), wetted perimeter $P$ (L), and free-surface width $L$ (L), the following parameters were obtained: mean flow depth $y_m$ ($y_m = A/L$); hydraulic radius $R$ ($R = A/P$); unit discharge $q$($L^2/T$); average flow velocity $U$ (L/T); Froude number of flow $Fr$ ($Fr = U/(gy_m)^{0.5}$); Reynolds number of flow $Re$ ($Re = U\,R/\nu$) with $\nu$ equal to the kinematic viscosity ($L^2/T$) ; dimensionless grain size $D_{gr}$ ($D_{gr} = d_{84}((g\Delta/\nu^2)^{1/3}$), with $\Delta$ = s−1 and $s = 2.65$; Shields sediment mobility parameter, suggested by Yalin (1972) $Y = u^{*2}/g\ d_{84}\ \Delta$; and, ratio between $Y$ and its critical value $Y_{cr}$ (0.029), proposed by Ackers and White (1973).

Finally, according to the equations given as (2), original Manning coefficient, Chezy coefficient, and Darcy-Weisbach friction factor were estimated for each cross section.

The initial data set was validated through different phases. First, to exclude vegetation effects on flow resistance, only river reaches without evident signs of vegetation in the different seasons of the year were considered. Then, with the aim of not allowing for at-a-site variation, only measurements whose roughness values, observed along a given reach during all the months of the sampling period and estimated by means of the equations given as (2), deviated from the average sample value by less than 20% for the Chezy, Darcy-Weisbach, and Manning equations were valued reliable.

These conditions reduced the database volume to 517 useful cross sections. Next, according to the characteristics of the ADV instrument, it was decided not to consider mean flow depth values less than 0.05 m (16 cross sections removed). Moreover, to satisfy gravel-bed conditions and following the Ackers and White method (1973) where coarse material with $D_{gr} \geq 60$ is considered to be moved as bed load, all the river

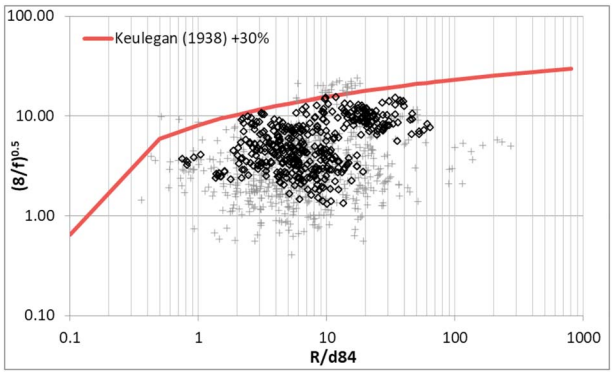


**Figure 2.** Validated data set of 409 field measurements (black rhombus) shown in terms of $(8/f)^{0.5}$ versus $R/d_{84}$. The grey crosses represent all the measurements not considered suitable for analysis.

reaches characterized by $D_{gr}$ values less than 60 were neglected (five cross sections removed). The data set was further cleaned, eliminating another 65 doubtful cross sections characterized both by low mean flow depth values (varying from 0.05 to 0.15 m) and by very high values of bed slope (varying from about 10% to about 20%)

Finally, in order to remove cross sections characterized by very flat beds, fine sands, and mild bed slopes, we proceeded with the criterion suggested by Rickenmann and Recking (2011), in which the observed data, shown in terms of $(8/f)^{0.5}$ and $R/d_{84}$, must be less than values 30% higher than those predicted with the Keulegan law (1938), thus removing 22 cross sections. The final data set of 409 observations, which was taken as a basis for the following analyses, is shown in Figure 2 in terms of $(8/f)^{0.5}$ and $R/d_{84}$, and it is also described in the supporting information Table S1 in terms of main geometric, granulometric, and hydraulic characteristics.

Specifically, in Table 1 are summarized some statistics for the hydraulic and sediment parameters related to the data set of the 409 observations, while in Figure 3 the corresponding frequency classes for the same parameters are shown. From a hydraulic point of view, it was observed that the Reynolds number of flow is ranging from $1.0 \times 10^4$ to $1.2 \times 10^6$ and that almost all the river reaches showed subcritical flow conditions with $Fr < 1$ (96.82%). Regarding the criteria for the selection of the amount of material moved as bed load, taking into account what was highlighted by MacKenzie et al. (2018), we decided to use four literature models as references, including those by Shields (1936), Yalin (1972), and Charlton et al. (1978), with the mobility condition occurring when $d_{50} < [(y_m\ S_f)/(0.04\Delta)]$, and Griffiths (1981), with the mobility condition occurring when $d_{50} < 11\ y_m\ S_f$. For each of these models, three flow domains were analyzed: *domain 1*, corresponding to river reaches characterized by no bed load; *domain 2*, corresponding to a moderate bed load transport rate; and *domain 3*, corresponding to high bed load transport rate. The transition from domains 1 to 2 was carried out considering for each method the corresponding critical value of the sediment mobility parameter. Regarding the passing from domains 2 to 3, the criterion suggested by Recking et al. (2008) has been adopted which sets this second threshold equal to about 2.5 the critical value. As a consequence, the river reaches characterized by sediment mobility parameter values ranging from 1 to 2.5 times the corresponding critical value were assigned to *domain 2*.

From an analysis of the sediment mobility parameters, similar behavior was observed for the Griffiths and Shields approaches, both with the 19.56% of river reaches in domain 1, the 29.58% in domain 2, and the 50.86% in domain 3. The parameter of Charlton et al. (1978) placed 12.22% of river reaches in domain 1, 27.38% in domain 2, and 60.40% in domain 3, while in the case of the Yalin index, we achieved 28.12% of river reaches in domain 1, 36.18% in domain 2, and 35.70% in domain 3. Considering field observations and the fact that some of these parameters were determined in different conditions from those characterizing gravel beds (Charlton et al., 1978; Shields, 1936), the sediment mobility parameter proposed by Yalin (1972) was selected for analysis, with its critical value $Y_{cr}$ (0.029) as defined by Ackers and White (1973).

A further classification, following Bathurst et al. (1981), regarded the subdivision of the data set into three relative submergence classes according to $R/d_{84}$, resulting in the percentages shown in Table 2. Based on

**Table 1**
*Ranges of Hydraulic and Sediment Parameters for the Whole Data Set Analyzed*

| | $S_f$ (m/m) | $d_{90}$ (mm) | $d_{84}$ (mm) | $d_{50}$ (mm) | $d_{16}$ (mm) | $Q$ ($m^3$/s) | $L$ (m) | $R$ (m) | $y_m$ (m) | $U$ (m/s) | $R/d_{84}$ (−) | $Fr$ (−) | $Y/Y_{cr}$ (−) | $D_{gr}$ (−) |
|---|---|---|---|---|---|---|---|---|---|---|---|---|---|---|
| Max Value | 0.1577 | 252.64 | 120.00 | 63.16 | 16.00 | 17.80 | 51.80 | 0.64 | 0.65 | 2.29 | 63.60 | 1.27 | 29.06 | 3015.44 |
| Min Value | 0.0007 | 7.50 | 5.80 | 0.24 | 0.04 | 0.01 | 0.80 | 0.05 | 0.05 | 0.16 | 0.75 | 0.17 | 0.16 | 145.75 |
| Mean Value | 0.0206 | 42.68 | 28.83 | 11.28 | 2.51 | 2.52 | 10.53 | 0.21 | 0.21 | 0.77 | 10.60 | 0.56 | 2.65 | 724.55 |
| Standard Deviation | 0.0233 | 40.93 | 20.51 | 10.75 | 3.40 | 3.25 | 10.30 | 0.12 | 0.12 | 0.32 | 10.14 | 0.18 | 2.89 | 515.43 |

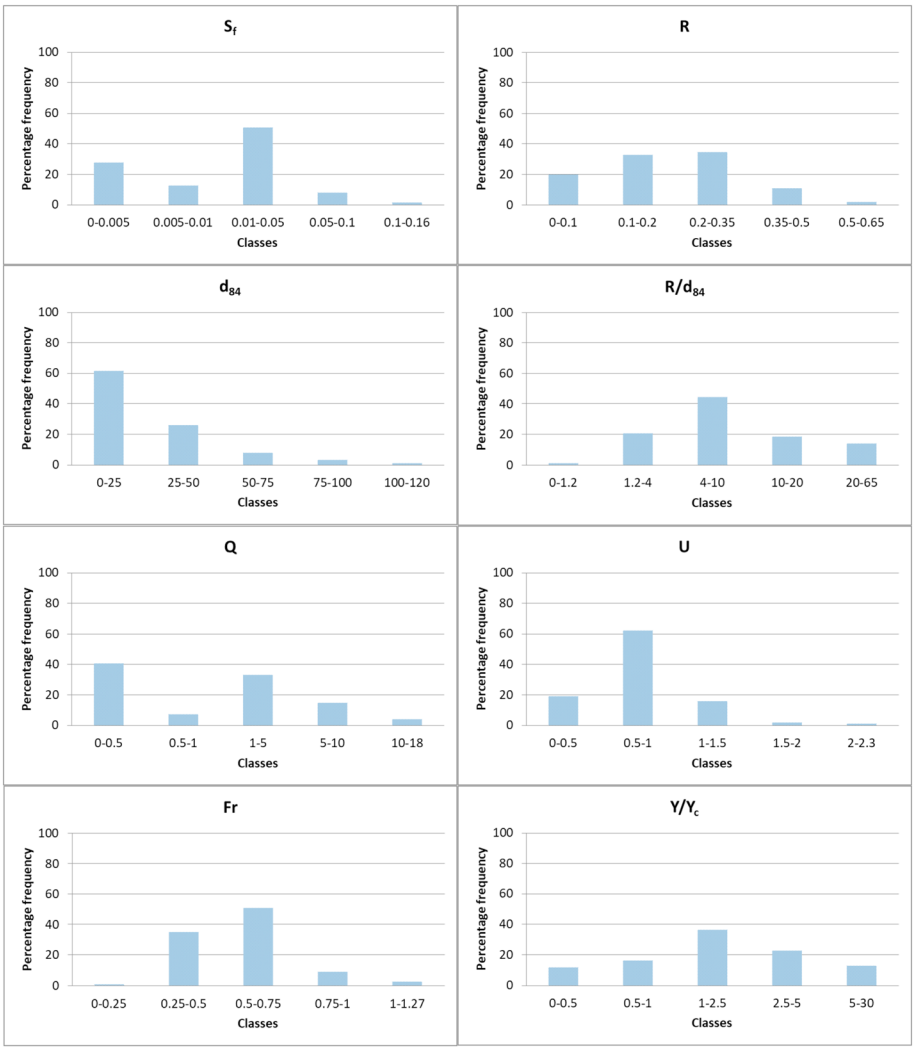


**Figure 3.** Frequency classes of hydraulic and sediment parameters for the whole data set analyzed.

the elements falling in each class, only two categories will be considered: small- and intermediate/large-scale roughness (only six measurements were characterized by $R/d_{84} < 1.2$).

In order to illustrate the data distribution in relation to bed load domains, as proposed by Yalin (1972) with the critical values $Y_{cr}$ (0.029) and Recking et al. (2008) with 2.5 $Y_{cr}$, also considering the Bathurst et al. (1981) subdivision into small-, intermediate-, and large-scale roughness, Figure 4 shows the whole Calabrian data set of 409 pairs of points ($1/S_f$ versus $R/d_{84}$), divided into the classes listed above.

**Table 2**
*Relative Submergence Classes $R/d_{84}$ (Bathurst et al., 1981) for the Whole Data Set Analyzed*

| Scale roughness | Data set Classes | 409 observations | |
|---|---|---|---|
| | | $n°$ | % |
| Large | $R/d_{84} < 1.2$ | 6 | 1.47 |
| Intermediate | $1.2 < R/d_{84} < 4$ | 85 | 20.78 |
| Small | $R/d_{84} > 4$ | 318 | 77.75 |

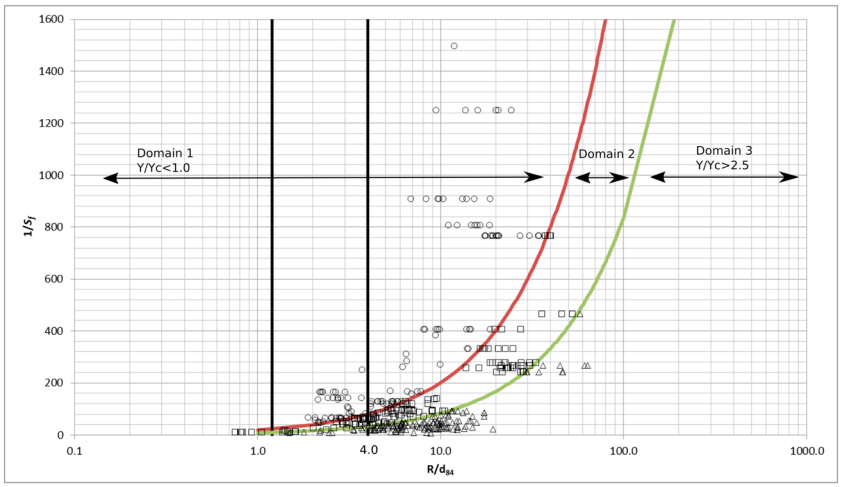


**Figure 4.** Calabrian data set of 409 pairs of points ($1/S_f$ versus $R/d_{84}$) divided according to the bed load conditions, as proposed by Yalin (1972) with the critical value $Y_{cr}$ (0.029) and Recking et al. (2008) with 2.5 $Y_{cr}$: black circles, domain 1; black squares, domain 2; and black triangles, domain 3. A further subdivision is also given by considering the Bathurst et al. (1981) small-, intermediate-, and large-scale roughness classes.

For the analyses next shown, the data set was divided into two subsets: a calibration subset and a validation one. The former (242 observations) was achieved according to the criterion suggested by Rickenmann and Recking (2011), in which the observed data, shown in terms of $(8/f)^{0.5}$ and $R/d_{84}$, must be both less than values 30% higher than those predicted with the Keulegan law (1938), and greater than values 30% lower than those predicted by the friction law of Recking et al. (2008):

$$\sqrt{\frac{8}{f}} = -1 + 9.5\ \log\left(\frac{R}{d_{84}}\right) \tag{15}$$

which is applied for very steep slopes and high sediment transport (enveloped black points data set of Figure 5). All measurements outside this last curve (167 observations represented by the grey points of Figure 5), mainly characterized by very high bed load transport rate and very steep slope (29% in domain 2, with 8% of this data very close to the limit of 2.5 $Y_{cr}$, and 71% in domain 3), were next considered for a first validation phase.

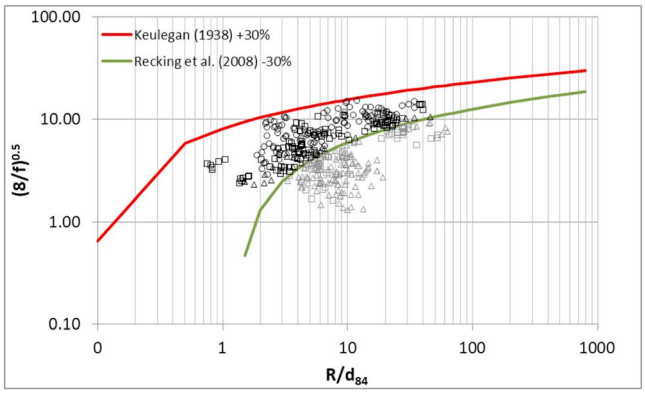


**Figure 5.** Field measurements shown in terms of $(8/f)^{0.5}$ versus $R/d_{84}$: black points) data set of 242 cross sections achieved according to the approach suggested by Rickenmann and Recking (2011) and considered for the calibration phase; grey points) data set of 167 cross sections used for a first validation phase. Both for black and grey points, circles represent the observations in the domain 1, squares represent the observations in the domain 2, and triangles represent the observations in the domain 3.

In Tables 3 and 4 are summarized some statistics for the hydraulic and sediment parameters related to the data set shown in Figure 5.

Furthermore, with the aim of guaranteeing that the sediment mobility parameter cannot indirectly take into account the effect of the Froude number on the flow resistance equations (Ferro, 1999), the correlation degree between $Y/Y_{cr}$ and $Fr$ for the whole data set and for its subsets obtained according to domains 1, 2, and 3 has been verified (see supporting information Figure S1), that is, there is no clear correlation.

Finally, to yield more general results, the validation procedure was extended (second validation phase) using another literature-based data set composed of about 2,000 field data from miscellaneous rivers. This data set represents a wide range of hydraulic and geomorphologic conditions in the field, ranging from coarse gravel-bed rivers and very steep rivers to nearly flat rivers. Table 5 shows the main hydraulic and sediment characteristics of the data gathered. This data set included flow data from subcritical (97%) to supercritical (3%) flow conditions and Reynolds number values ranging from $3.6 \times 10^3$ to $3.3 \times 10^7$. Channel slopes range from 0.0001% to 24% or from nearly flat rivers to rivers characterized by very

**Table 3**
*Ranges of Hydraulic and Sediment Parameters for the Black Points Data Set Shown in Figure 5*

| | $S_f$ (m/m) | $d_{90}$ (mm) | $d_{84}$ (mm) | $d_{50}$ (mm) | $d_{16}$ (mm) | $Q$ ($m^3$/s) | L (m) | $R$ (m) | $y_m$ (m) | $U$ (m/s) | $R/d_{84}$ (−) | $Fr$ (−) | $Y/Y_{cr}$ (−) | $D_{gr}$ (−) |
|---|---|---|---|---|---|---|---|---|---|---|---|---|---|---|
| Max Value | 0.1020 | 252.64 | 120.00 | 63.16 | 16.00 | 17.80 | 51.80 | 0.56 | 0.58 | 2.29 | 46.47 | 1.27 | 5.98 | 3015.44 |
| Min Value | 0.0007 | 12.70 | 6.80 | 1.80 | 0.06 | 0.01 | 0.80 | 0.05 | 0.05 | 0.28 | 0.75 | 0.25 | 0.16 | 170.88 |
| Mean Value | 0.0170 | 54.14 | 34.96 | 14.15 | 3.35 | 2.91 | 12.02 | 0.21 | 0.22 | 0.85 | 9.06 | 0.62 | 1.32 | 878.60 |
| Standard Deviation | 0.0232 | 49.06 | 23.10 | 12.46 | 4.09 | 3.24 | 11.14 | 0.12 | 0.13 | 0.34 | 8.72 | 0.18 | 1.01 | 580.35 |

steep slopes through a series of bed channel bed morphologies. Regarding the grain size, $d_{50}$ ranges from 0.028 to 650 mm and $d_{84}$ ranges from 0.07 to 1,350 mm. If the grain size $d_{84}$ was missing, it was estimated by 2.5 $d_{50}$. This approximation, based on the median value for 1,000 pairs of $d_{50}$ and $d_{84}$ values available within the literature-based data set (50% of the whole data set), agrees with $d_{84} = 2.2\ d_{50}$ achieved by Rickenmann and Recking (2011). For the estimate of the hydraulic radius, when it was not present, a rectangular cross section has been hypothesized, according to the method used by Rickenmann and Recking (2011). As previously, observed data 30% higher than those predicted with the Keulegan law (1938), together with river reaches characterized by $D_{gr}$ values less than 60, were removed from the whole data set (grey crosses of Figure 6). According to Bathurst et al. (1981), the final literature-based data set of 1,757 pairs of points was also subdivided into two subsets: a calibration subset, including 708 cross sections characterized by large-scale roughness (black rhombus of Figure 6), and a validation subset including 357 cross sections characterized by intermediate-scale roughness and 692 cross sections characterized by small-scale roughness (black rectangles of Figure 6).

## 4. Comparison of Flow Resistance Equations

The data set of Figure 5 was used to verify the performances of the main flow resistance equations shown in section 2. The equations of Strickler (1923; equation (3)), Limerinos (1970; equation (4)), Jarrett (1984; equation (5)), Keulegan (1938; equation (6)), Hey (1979; equation (6) with $k_s = 3.5d_{84}$), Bathurst (1985; equation (7)), Smart and Jaeggi (1983; equation (8)), Chow (1959; equation (9)), Ferguson (2007; equation (13)), and Rickenmann and Recking (2011; equation (14)) were analyzed and plotted for comparison in terms of $(8/f)^{0.5}$ versus $R/d_{84}$, within the enveloping laws of Figure 5 (supporting information Figure S2). This envelope appears useful to understand a first estimation of the reliability of the single equations both in relative and absolute terms; for example, in the field of small-scale roughness, the Keulegan equation predicts flow velocities 30% higher than the Hey equation, and when the relative submergence decreases (large-scale roughness), this ratio increases reaching 100%. As well, the envelope points out the reduced capability of all equations when the flow resistance in river reaches characterized by high bed load transport rate (grey points of Figure 5) is estimated.

To measure the performances of the equations, four statistical indices were used: the squared correlation coefficient $R^2$; two error indices, defined as the root mean square error ($RMSE$) and the scatter index ($SI$):

**Table 4**
*Ranges of Hydraulic and Sediment Parameters for the Grey Points Data Set Shown in Figure 5*

| | $S_f$ (m/m) | $d_{90}$ (mm) | $d_{84}$ (mm) | $d_{50}$ (mm) | $d_{16}$ (mm) | $Q$ ($m^3$/s) | $L$ (m) | $R$ (m) | $y_m$ (m) | $U$ (m/s) | $R/d_{84}$ (−) | Fr (−) | $Y/Y_{cr}$ (−) | $D_{gr}$ (−) |
|---|---|---|---|---|---|---|---|---|---|---|---|---|---|---|
| Max Value | 0.1577 | 63.00 | 50.00 | 19.50 | 6.70 | 16.32 | 41.80 | 0.64 | 0.65 | 1.27 | 63.60 | 1.00 | 29.06 | 1256.44 |
| Min Value | 0.0021 | 7.50 | 5.80 | 0.24 | 0.04 | 0.01 | 0.80 | 0.05 | 0.05 | 0.16 | 3.38 | 0.17 | 1.13 | 145.75 |
| Mean Value | 0.0260 | 26.07 | 19.95 | 7.11 | 1.29 | 1.96 | 8.37 | 0.20 | 0.20 | 0.66 | 12.83 | 0.48 | 4.59 | 501.31 |
| Standard Deviation | 0.0224 | 12.40 | 11.20 | 5.41 | 1.27 | 3.18 | 8.52 | 0.11 | 0.11 | 0.25 | 11.57 | 0.14 | 3.57 | 281.54 |

Water Resources Research

10.1029/2019WR024819

**Table 5**
*Ranges of Hydraulic and Sediment Parameters for the Literature-Based Data Set*

| Reference | $L$ (m) | $S_f$ (m/m) | $Q$ (mc/s) | $y_m$ (m) | $R$ (m) | $U$ (m/s) | $d_{50}$ (m) | $d_{84}$ (m) | N |
|---|---|---|---|---|---|---|---|---|---|
| Adenlof and Wohl (1994) | 2.10–5.40 | 0.058–0.197 | 0.52–0.98 | 0.19–0.35 | NA | 0.55–1.07 | NA | 0.056–0.121 | 12 |
| Andrews (1994) | 2.57 | 0.0095–0.011 | 0.99–3.12 | 0.35–1.59 | NA | 1.103–1.957 | 0.058 | 0.104 | 55 |
| Bathurst (1985) | 5.07–49.80 | 0.00398–0.0373 | 0.137–195 | 0.10–1.6 | NA | 0.34–3.72 | 0.060–0.387 | 0.113–0.740 | 44 |
| Bray (1979) | 14.33–544.68 | 0.00022–0.015 | 5.52–8207 | NA | 0.44–6.92 | 0.49–2.77 | 0.012–0.145 | NA | 67 |
| Charlton et al. (1978) | 5.24–59.35 | 0.0007–0.0137 | 2.7–550 | 0.65–4.19 | NA | 0.79–2.55 | 0.028–0.113 | 0.045–0.269 | 23 |
| Church and Rood (1983) | 2–900 | 0.00004–0.081 | 0.06–16.95 | 0.04–13.92 | NA | 0.09–4.70 | 0.00015–0.268 | NA | 495 |
| Colosimo et al. (1988) | 3–23.0 | 0.0026–0.019 | 0.4–17.9 | 0.26–0.58 | NA | 0.43–2.71 | 0.021–0.063 | NA | 43 |
| David et al. (2010) | 5.9–35.5 | 0.017–0.195 | 0.01–1.85 | NA | 0.05–0.26 | 0.11–2.07 | 0.010–0.080 | 0.050–0.170 | 30 |
| Ferro and Porto (2018) | NA | 0.0071–0.0619 | NA | 0.08–0.33 | 0.08–0.54 | 0.28–1.07 | 0.007–0.119 | 0.013–0.228 | 59 |
| Griffths (1981) | 2.9–123 | 0.000095–0.011 | 0.05–1540 | NA | 0.12–6.89 | 0.09–3.32 | 0.013–0.301 | NA | 84 |
| Hey and Thorne (1986) | 5.5–77.1 | 0.00119–0.021 | 3.9–424 | 0.50–3.21 | 0.48–3.1 | 0.89–3.0 | 0.014–0.1758 | NA | 62 |
| Hey (1979) | NA | 0.0009–0.031 | 0.995–189.82 | NA | 0.141–2.23 | 0.27–2.31 | NA | 0.046–0.250 | 17 |
| Jarrett (1984) | 6.70–51.83 | 0.002–0.034 | 0.34–128.29 | 0.14–2.00 | 0.15–1.68 | 0.27–2.64 | 0.015–0.426 | 0.038–0.792 | 75 |
| Jones and Seitz (1979) | 134.15–185.97 | 0.000183–0.00098 | 0.67–2.32 | 3.90–4.97 | NA | 1.29–2.68 | 0.00036–0.043 | 0.00052–0.083 | 22 |
| Leopold and Emmett (1976) | 14.6 | 0.0007 | 2.44–41.5 | 0.28–2.01 | NA | 0.61–1.41 | 0.00041–0.00176 | NA | 140 |
| Nakato et al. (1977) | NA | 0.000001–0.000307 | NA | NA | 1.04–5.67 | 0.04–1.11 | 0.00032–0.00076 | NA | 45 |
| Orlandini et al. (2006) | 1.5–8.8 | 0.028–0.181 | 0.017–0.775 | 0.17–0.37 | NA | 0.07–0.51 | NA | 0.249–0.963 | 12 |
| Pemberton (1964) | NA | 0.00085–0.0009 | NA | NA | 0.50–0.74 | 0.75–1.72 | 0.000254–0.0005 | NA | 6 |
| Reid and Hickin (2008) | 1.7–20.45 | 0.017–0.075 | 0.029–5.523 | 0.06–0.54 | NA | 0.03–1.08 | 0.105–0.190 | 0.200–0.570 | 619 |
| Simons and Albertson (1960) | NA | 0.000058–0.000388 | NA | NA | 0.55–2.04 | 0.41–0.78 | 0.000028–0.000805 | NA | 22 |
| Thompson and Campbell (1979) | 4.7–55.4 | 0.0037–0.052 | 2.7–410.6 | NA | 0.25–2.62 | 0.92–3.02 | 0.030–0.470 | NA | 22 |
| Thorne and Zevenbergen (1985) | 10.3–18.9 | 0.143–0.198 | 2.05–10.45 | 0.30–0.64 | NA | 0.52–1.42 | NA | 0.336–0.394 | 12 |
| Wohl and Wilcox (2005) | 2.2–38 | 0.003–0.24 | 1.3–193.8 | 0.2–1.9 | 0.21–0.19 | 1.0–3.6 | 0.038–0.65 | 0.14–1.35 | 34 |

*Note*. N = number of measurements; NA = not applicable.

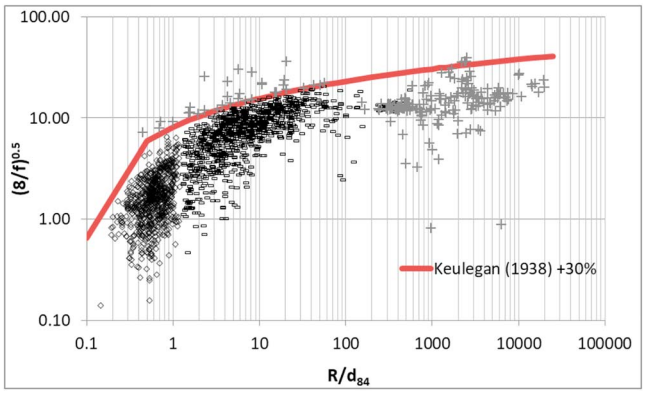


**Figure 6.** $(8/f)^{0.5}$ versus $R/d_{84}$ values calculated on the basis of literature data shown in Table 5. The grey crosses represent the pairs of points not considered for analysis purposes; the black rhombus represent the 708 pairs of points characterized by large-scale roughness and used for the second calibration phase, and the black rectangles represent the 1,049 pairs of points characterized by small- and intermediate-scale roughness and used for the second validation phase.

$$RMSE = \sqrt{\frac{\sum_{i=1}^{n}(x_i - y_i)^2}{n}} \tag{16}$$

$$SI = 100\,\frac{\sqrt{\left(\frac{1}{n}\right)\sum_{i=1}^{n}(x_i - y_i)^2}}{\overline{x}} \tag{17}$$

and; an index of agreement ($IA$):

$$IA = 1 - \frac{\sum_{i=1}^{n}(x_i - y_i)^2}{\sum_{i=1}^{n}\left(|x_i - \overline{x}| + |y_i - \overline{y}|\right)^2} \tag{18}$$

where $\overline{x}$ is the mean of the $n$ observed $x_i$ values and $\overline{y}$ is the mean of the $n$ calculated $y_i$ values.

The performance of each considered equation was verified by estimating the average flow velocity using the whole enveloped black points data set of Figure 5 (supporting information Figure S3). The statistical indices values (Table 6) showed for all the equations not high performances, which in general tend to increase according to higher relative submergence values (i.e., passing from intermediate- to small-scale roughness). The box plots shown in Figure 7, obtained considering the ratio of calculated to observed flow velocity values for different $R/d_{84}$ classes, pointed out a significant overestimation of the $U$ values for the Strickler, Keulegan, and Iwagaki-Chow equations, while a marked underestimation occurs for the Jarrett equation. In the remaining equations, for relative submergence values ranging from 1.2 to 8 (intermediate- and small-scale roughness), a general overestimation (more limited than that found for the previous equations) is observed. For $R/d_{84}$ values greater than 8 (very small-scale roughness), the same equations have shown good performance with alternating under-over estimates. In the field of the large-scale roughness ($R/d_{84}$ values <1.2), unlike the good performance provided by the Bathurst equation, a trend inversion is detected for flow velocity values greater than 1.5 m/s, and high $U$ values are significantly underestimated.

In order to understand the main sources of error found in the previous analysis, following Gao and Abrahams (2004), Recking et al. (2008), and Ferro (2018b) about the effects induced by the bed load transport on flow resistance, first we analyzed only the measurements characterized by no bed load transport rate, corresponding to the enveloped black circles data set of Figure 5 with the ratio $Y/Y_{cr} < 1$, then we used the measurements characterized by very high bed load transport rate, corresponding to the grey points data set (squares and triangles) of the same figure.

As pointed out in Table 6, all the equations showed an improvement in performance when no bed load transport is observed. Also, in the case of the Jarrett equation, even though a lower $R^2$ value is obtained, decreasing from 0.56 to 0.50, it is possible to observe that the other statistical indices show better behavior for this condition. For measurements characterized by very high values of the ratio $Y/Y_{cr}$, all the equations showed a substantial reduction in performance indicating a substantial increase in the overestimation of flow velocities, more evident for relative submergence values close to 10, as well as reported in Table 6 and in the supporting information Figure S4. This last figure shows that none of these equations for estimating a flow resistance coefficient is designed specifically for very high values of bed load transport rate and steep channels. Only the Jarrett equation, just because obtained for river flows characterized by high energy dissipations, allows determining for all the considered relative submergence classes acceptable flow velocity values, significantly reducing the underestimation observed in the previous analysis.

Again, in order to identify the individual factors contributing to significant variation in the equations' performance, Table 6 shows the results obtained considering the enveloped black circles data set, characterized by the ratio $Y/Y_{cr} < 1$, subdivided according to small- and intermediate/large- scale roughness. In this context, it is useful to divide the flow resistance equations into three groups: equations whose performance

**Table 6**
*Performances of the Considered Equations in the Estimation of Average Flow Velocity Using the Whole Enveloped Black Points Data Set in Figure 5 and Its Subsets Relative to River Reaches Characterized by No Bed Load Transport Rate and to Small- or Intermediate/Large-Scale Roughness, as Well as the Grey Points Data Set in Figure 5*

| Equation | Black points: Whole data set N. 242 | Black circles: No bed load transport ($Y/Y_{cr} < 1$) N. 115 | Black circles: ($Y/Y_{cr} < 1$) interm./large roughness N. 40 | Black circles: ($Y/Y_{cr} < 1$) small roughness N. 75 | Grey points ($Y/Y_{cr} >> 1$): Whole data set N. 167 |
|---|---|---|---|---|---|
| Strickler (1923) | $R^2 = 0.29$ | $R^2 = 0.54$ | $R^2 = 0.51$ | $R^2 = 0.67$ | $R^2 = 0.18$ |
| | $RMSE = 0.72$ | $RMSE = 0.36$ | $RMSE = 0.48$ | $RMSE = 0.28$ | $RMSE = 1.74$ |
| | $SI = 85.15$ | $SI = 47.97$ | $SI = 68.24$ | $SI = 35.86$ | $SI = 263.27$ |
| | $IA = 0.26$ | $IA = 0.68$ | $IA = 0.63$ | $IA = 0.73$ | $IA = -2.16$ |
| Limerinos (1970) | $R^2 = 0.49$ | $R^2 = 0.65$ | $R^2 = 0.61$ | $R^2 = 0.70$ | $R^2 = 0.23$ |
| | $RMSE = 0.29$ | $RMSE = 0.18$ | $RMSE = 0.25$ | $RMSE = 0.14$ | $RMSE = 1.08$ |
| | $SI = 34.49$ | $SI = 24.32$ | $SI = 35.10$ | $SI = 17.79$ | $SI = 164.48$ |
| | $IA = 0.81$ | $IA = 0.88$ | $IA = 0.86$ | $IA = 0.90$ | $IA = -1.04$ |
| Jarrett (1984) | $R^2 = 0.56$ | $R^2 = 0.50$ | $R^2 = 0.72$ | $R^2 = 0.40$ | $R^2 = 0.52$ |
| | $RMSE = 0.45$ | $RMSE = 0.36$ | $RMSE = 0.44$ | $RMSE = 0.31$ | $RMSE = 0.24$ |
| | $SI = 53.29$ | $SI = 48.10$ | $SI = 64.38$ | $SI = 39.56$ | $SI = 36.93$ |
| | $IA = 0.24$ | $IA = 0.41$ | $IA = 0.40$ | $IA = 0.30$ | $IA = 0.64$ |
| Keulegan (1938) | $R^2 = 0.30$ | $R^2 = 0.55$ | $R^2 = 0.51$ | $R^2 = 0.66$ | $R^2 = 0.17$ |
| | $RMSE = 1.00$ | $RMSE = 0.56$ | $RMSE = 0.67$ | $RMSE = 0.50$ | $RMSE = 2.27$ |
| | $SI = 118.95$ | $SI = 74.61$ | $SI = 95.53$ | $SI = 64.44$ | $SI = 344.31$ |
| | $IA = -0.133$ | $IA = 0.38$ | $IA = 0.40$ | $IA = 0.34$ | $IA = -2.83$ |
| Hey (1979) | $R^2 = 0.50$ | $R^2 = 0.65$ | $R^2 = 0.62$ | $R^2 = 0.70$ | $R^2 = 0.23$ |
| | $RMSE = 0.28$ | $RMSE = 0.18$ | $RMSE = 0.25$ | $RMSE = 0.14$ | $RMSE = 1.07$ |
| | $SI = 33.67$ | $SI = 24.47$ | $SI = 35.38$ | $SI = 17.82$ | $SI = 165.60$ |
| | $IA = 0.81$ | $IA = 0.88$ | $IA = 0.86$ | $IA = 0.90$ | $IA = -1.01$ |
| Bathurst (1985) | $R^2 = 0.48$ | $R^2 = 0.64$ | $R^2 = 0.61$ | $R^2 = 0.70$ | $R^2 = 0.22$ |
| | $RMSE = 0.35$ | $RMSE = 0.19$ | $RMSE = 0.25$ | $RMSE = 0.15$ | $RMSE = 1.22$ |
| | $SI = 41.98$ | $SI = 24.99$ | $SI = 35.33$ | $SI = 18.86$ | $SI = 185.16$ |
| | $IA = -0.74$ | $IA = 0.89$ | $IA = 0.87$ | $IA = 0.90$ | $IA = -1.30$ |
| Smart and Jaeggi (1983) | $R^2 = 0.39$ | $R^2 = 0.46$ | $R^2 = 0.45$ | $R^2 = 0.60$ | $R^2 = 0.31$ |
| | $RMSE = 0.32$ | $RMSE = 0.23$ | $RMSE = 0.32$ | $RMSE = 0.16$ | $RMSE = 1.14$ |
| | $SI = 37.45$ | $SI = 29.96$ | $SI = 45.49$ | $SI = 19.84$ | $SI = 172.20$ |
| | $IA = 0.76$ | $IA = 0.80$ | $IA = 0.68$ | $IA = 0.87$ | $IA = -1.17$ |
| Iwagaki-Chow (1959) | $R^2 = 0.39$ | $R^2 = 0.57$ | $R^2 = 0.54$ | $R^2 = 0.66$ | $R^2 = 0.17$ |
| | $RMSE = 0.82$ | $RMSE = 0.49$ | $RMSE = 0.57$ | $RMSE = 0.44$ | $RMSE = 2.00$ |
| | $SI = 97.63$ | $SI = 64.80$ | $SI = 81.68$ | $SI = 55.91$ | $SI = 302.93$ |
| | $IA = 0.11$ | $IA = 0.52$ | $IA = 0.55$ | $IA = 0.47$ | $IA = -2.59$ |
| Ferguson (2007) | $R^2 = 0.52$ | $R^2 = 0.64$ | $R^2 = 0.64$ | $R^2 = 0.70$ | $R^2 = 0.22$ |
| | $RMSE = 0.27$ | $RMSE = 0.19$ | $RMSE = 0.26$ | $RMSE = 0.14$ | $RMSE = 1.06$ |
| | $SI = 31.50$ | $SI = 25.66$ | $SI = 37.70$ | $SI = 18.17$ | $SI = 160.97$ |
| | $IA = 0.84$ | $IA = 0.87$ | $IA = 0.83$ | $IA = 0.90$ | $IA = -0.96$ |
| Rickenmann and Recking (2011) | $R^2 = 0.49$ | $R^2 = 0.65$ | $R^2 = 0.63$ | $R^2 = 0.69$ | $R^2 = 0.20$ |
| | $RMSE = 0.32$ | $RMSE = 0.18$ | $RMSE = 0.24$ | $RMSE = 0.15$ | $RMSE = 1.17$ |
| | $SI = 37.96$ | $SI = 24.33$ | $SI = 33.73$ | $SI = 18.87$ | $SI = 176.82$ |
| | $IA = 0.79$ | $IA = 0.89$ | $IA = 0.88$ | $IA = 0.90$ | $IA = -1.16$ |

*Note*. N = number of measurements.

improves only in the case of small-scale roughness, equations whose performance improves only in the case of intermediate/large-scale roughness, and equations whose performance is acceptable for both roughness scales.

The Strickler equation (with $R^2 = 0.67$, $RMSE = 0.28$, $SI = 35.86$, and $IA = 0.73$) and the Smart and Jaeggi equation (with $R^2 = 0.60$, $RMSE = 0.16$, $SI = 19.84$, and $IA = 0.87$) belong to the first group. Equations in the second group are not clearly observed. The Limerinos, Hey, Bathurst, Ferguson, and Rickenmann and Recking equations showed the best performance for river reaches characterized by small-scale roughness, but they can also be used (achieving slightly lower performance) for river reaches characterized by intermediate/large-scale roughness. This result, in close agreement with studies carried out by Ferguson (2007) and Rickenmann and Recking (2011), leads to a reassessment of the use of equations such as those

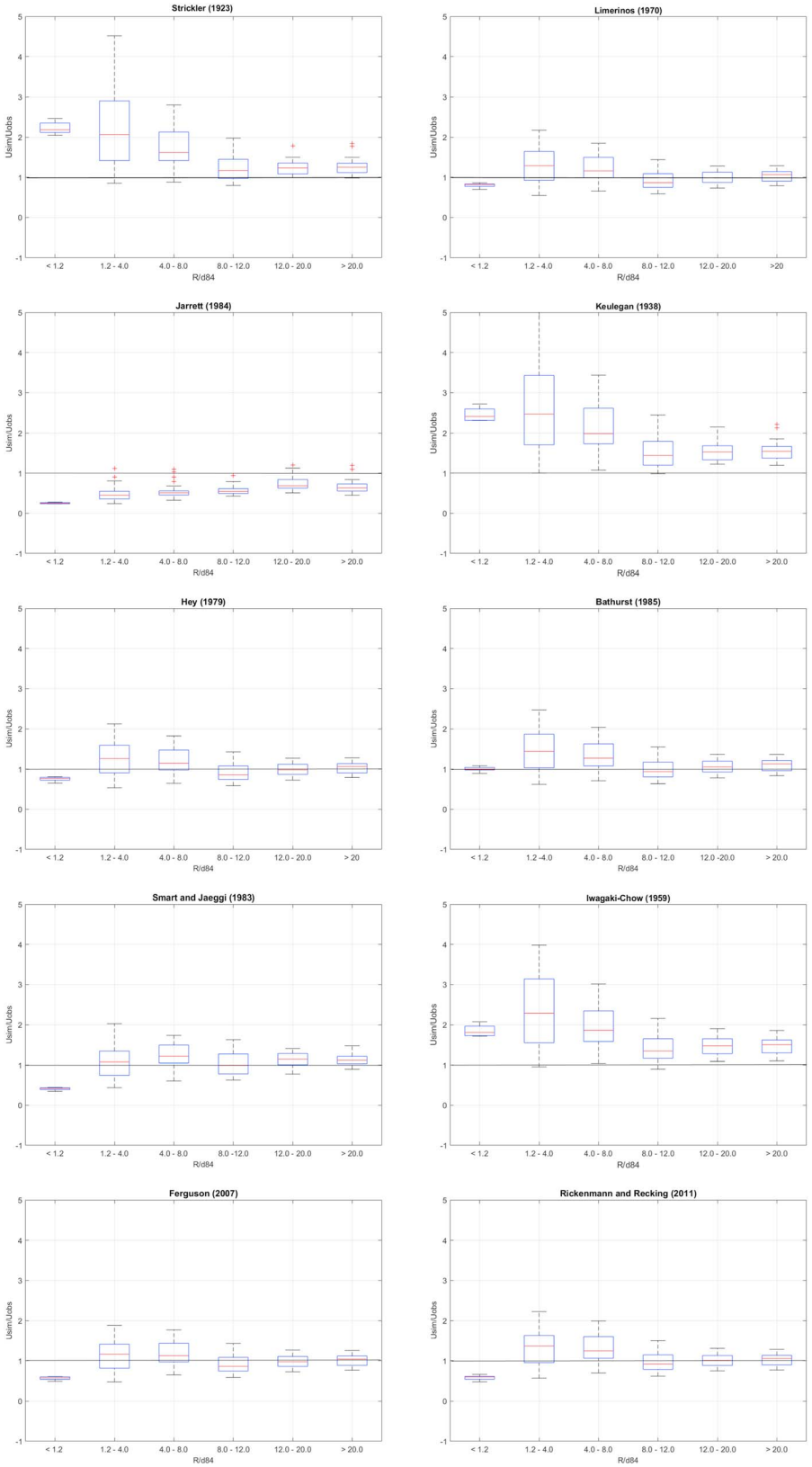


**Figure 7.** Results for the ratio of simulated to observed flow velocity values and shown for different $R/d_{84}$ classes using the whole enveloped black points data set of Figure 5. (top to bottom) Values in box plots correspond to the maximum, third quartile, median, first quartile, and minimum.

proposed by Limerinos, Hey, and Bathurst. In fact, these equations show statistical indices values for river reaches characterized by small-scale roughness equal to those achieved using the Ferguson and Rickenmann and Recking equations. Moreover, it is interesting to note that for river reaches characterized by intermediate/large-scale roughness, while the best performance is observed for the Rickenmann and Recking equation (with $R^2 = 0.63$, $RMSE = 0.24$, $SI = 33.73$, and $IA = 0.88$), the Bathurst, Hey, and Limerinos equations not only yield very similar values to the former equation but also provide a higher performance than the Ferguson equation (with $R^2 = 0.64$, $RMSE = 0.26$, $SI = 37.70$, and $IA = 0.83$).

Moreover, it is worth highlighting the particular behavior of the Keulegan, Iwagaki-Chow, and Jarrett equations: Although an increase in performance was shown for no bed load conditions, due to the discrepancy in the statistical indices, they do not demonstrate clear behavior that would indicate an optimal roughness scale for use.

In general, from the analysis just shown, it appears that the equations in Table 6, when applied in their original form to both the whole data set and subsets of homogeneous data, result in limited, though acceptable, performances, with the best statistical indices values equal to approximately $R^2 = 0.70$, $RMSE = 0.14$, $SI = 17.79$, and $IA = 0.90$.

This result led us to investigate new types of equations in which further dissipative contributions due to free surface instabilities, hydraulic jumps, and sediment transport dynamics can be explicitly evaluated through synthetic parameters and introduced in the estimation of flow resistance in natural rivers.

## 5. Influence of the Reynolds Number, Froude Number, and Sediment Mobility Parameter on Flow Resistance Equations

The results obtained so far point out the need to evaluate additional energy losses for a more accurate estimate of the flow resistance, such as already highlighted by Iwagaki (Chow, 1959), Rouse et al. (1963), Bathurst et al. (1981), Bathurst (1982), Graf et al. (1983), Colosimo et al. (1988, 1991), Rosso et al. (1990), Camacho and Yen (1991), Ugarte Soto and Madrid-Aris (1994), Baiamonte and Ferro (1997), Lawrence (1997), Afzalimehr and Anctil (1998), Ferro (2003), Dìaz (2005), Zhang et al. (2010), Wang and Dawdy (2014), Ferro (2017), Ferro (2018a), Di Stefano et al. (2018), and Ferro and Porto (2018). More specifically, starting from the researches carried out by Colosimo et al. (1988, 1991) a functional relationship for a straight channel with no vegetation was obtained using the Riabucinski-Buckingham theorem in a form such as this

$$\sqrt{\frac{8}{f}} = \boldsymbol{f}\left(Re, Fr, \frac{R}{d_{84}}, \quad \frac{L_f}{d_{84}}, \frac{L_t}{d_{84}}\Gamma, Y\right) \tag{19}$$

where $Re$ is the flow Reynolds number, $Fr$ is the flow Froude number, $\Gamma$ is the concentration of coarser elements (parameter that provides a measure of the frequency of the coarser elements in the bed layer), $Y$, $R$ and $d_{84}$ have the same meaning as defined above, $L_f$ is a parameter taking into account the longitudinal distance between the coarser bed elements, and $L_t$ is a parameter considering the transverse distance between the coarser bed elements measured in the cross-sectional plane. $L_f$ and $L_t$ provide information about the arrangement of the coarser bed particles and can be considered measures of the interference among the eddies with horizontal and vertical axis respectively, generated by the roughness elements. According to equation (19), Baiamonte and Ferro (1997) verified that if a detailed characterization of roughness geometry is determined, then the differences between observed and simulated $(8/f)^{0.5}$ values are due to Reynolds number, Froude number, and Shields sediment mobility parameter.

Concerning the Reynolds number, well-cited studies assume that the protrusion of the large roughness elements into the flow may cause a significant increase in the form drag, and if this last is considered to be the dominant factor for the evaluation of resistance induced by the large-scale roughness, then the dependence of the friction factor on the Reynolds number can be assumed negligible. Graf (1984) verified that for a gravel-bed channel $Re$ is so high that it does not influence the friction factor. Bray (1979), Hey (1979), Colosimo et al. (1988), and Baiamonte and Ferro (1997) showed that the friction factor is independent of the Reynolds number when $3.9 \times 10^4 < Re < 5.1 \times 10^5$. For rivers with gravel bed in mountainous region, Lawrence (1997) observed that, if the Reynolds number is greater than $10^4$, the effect of $Re$ can be easily

neglected. In fact, the same author underlines that the dependence on the Reynolds number can be very small because the flow is either partially or slightly inundated or is fully disturbed by the surface roughness so that the flow regime is similar to turbulent pipe flow in which roughness dominates. However, Bathurst et al. (1981) suggested that the Reynolds number can affect the flow resistance in the transitional region ($3.0 \times 10^4 < Re < 2.0 \times 10^5$), because in this region the drag coefficient of the bed element decreases when Re increases. This hypothesis agrees with the recent studies carried out by Cheng et al. (2016) and Ferro and Porto (2018), in which the effect of the Reynolds number on the flow resistance induced by large-scale roughness characterized by $1.0 \times 10^4 < Re < 5.0 \times 10^5$ may not really be negligible. According to the Reynolds number values shown by our data set ($1.0 \times 10^4 < Re < 1.2 \times 10^6$), we decided to investigate how the flow resistance is affected by flow regime ($Re$), flow condition ($Fr$), and sediment load ($Y/Y_{cr}$) and which of these parameters can better explain additional flow resistance contributions.

### 5.1. Proposal of New Resistance Equations

In our study, not limiting the analysis to the friction factor $f$ alone but also considering the $n$ and $C$ coefficients to represent the grain resistance, we investigated the benefits produced by the Froude number, the Reynolds number, and the ratio between the Shields sediment mobility parameter (1936), suggested by Yalin $Y$ (1972), and its critical value $Y_{cr}$, proposed by Ackers and White (1973), on four different flow resistance equations: Limerinos (1970), Hey (1979), Iwagaki-Chow (1959), and Rickenmann and Recking (2011). Specifically, to the original structure of the four flow resistance equations the term $\boldsymbol{f}(Y/Y_{cr}, Fr, Re)$ was added such as follows:

$$\boldsymbol{f}\left(\frac{Y}{Yc}, Fr, Re\right) = \left(b_1 \left(\frac{Y}{Y_{cr}}\right)^{b_2} Fr^{b_3} Re^{b_4}\right) + b_5 \tag{20}$$

with $b_1$, $b_2$, $b_3$, $b_4$, and $b_5$ coefficients obtained through calibration phases. From a mathematical point of view, different forms were hypothesized for the additional term $\boldsymbol{f}(Y/Y_{cr}, Fr, Re)$ and equation (20) while showing a fairly simple mathematical structure provided the best performance. It is useful to point out that in the case of Iwagaki-Chow (1959) the additional contribution was directly introduced in the coefficient $A_r$ according to the following scheme:

$$\mathrm{Ar} = \left(b_1 \left(\frac{Y}{Y_{cr}}\right)^{b_2} Fr^{b_3} Re^{b_4}\right) + b_5 \tag{21}$$

The coefficients of equations (20) and (21) were obtained by minimizing the differences between the 242 pairs of observed and calculated flow velocity values achieved by the measurements corresponding to the enveloped black points data set of Figure 5. Table 7 shows these coefficients for each considered equation, together with the statistical indices values indicating the improvement of the performances due to the combined action of $Fr$, $Re$, and the ratio $Y/Y_{cr}$.

Starting from the very low values assumed by the coefficient $b_4$ of Table 7, we assumed to neglect the Reynolds number within the corrective functions (20) and (21) in order to verify its effect on the flow resistance estimation and, then assuming as corrective function the following term $\boldsymbol{f}(Y/Y_{cr}, Fr)$:

$$\boldsymbol{f}\left(\frac{Y}{Yc}, Fr\right) = \left(b_1 \left(\frac{Y}{Y_{cr}}\right)^{b_2} Fr^{b_3}\right) + b_5 \tag{22}$$

and

$$\mathrm{Ar} = \left(b_1 \left(\frac{Y}{Y_{cr}}\right)^{b_2} Fr^{b_3}\right) + b_5 \tag{23}$$

Through a new calibration of the equations (22) and (23), achieved on the same 242 pairs of measurements corresponding to the enveloped black points data set of Figure 5, with the new coefficients and statistical indices values shown in Table 8, it was observed that the performances obtained with the (22) and (23)

**Table 7**
*Coefficients of the Proposed Equations f ($Y/Y_{cr}$, Fr, Re) and Corresponding Statistics Obtained Calibrating the Enveloped Black Points Data Set in Figure 5*

| | | | | | | Calibration | | | |
|---|---|---|---|---|---|---|---|---|---|
| Equation | $b_1$ | $b_2$ | $b_3$ | $b_4$ | $b_5$ | $R^2$ | RMSE | SI | IA |
| Limerinos | 0.10 | 0.33 | −0.57 | −0.07 | −0.05 | 0.90 | 0.12 | 14.80 | 0.97 |
| Hey | 9.43 | −0.25 | 0.38 | 0.03 | −12.00 | **0.93** | **0.10** | **11.30** | **0.98** |
| Iwagaki-Chow | 10.57 | −0.23 | 0.35 | 0.03 | −10.00 | **0.93** | **0.10** | 11.39 | **0.98** |
| Rickenmann and Recking | 9.36 | −0.25 | 0.37 | 0.03 | −12.00 | 0.87 | 0.14 | 16.00 | 0.96 |

*Note*. The bold values represent the best statistical indices values.

were slightly less than the previous (20) and (21) and that these differences were not so marked as to justify the Reynolds number within the additional term. Next, the same analysis was carried out, first, by neglecting *Fr* and leaving *Re* and the ratio $Y/Y_{cr}$ and, then, by neglecting the ratio $Y/Y_{cr}$ and leaving *Fr* and *Re*. These results provided performances significantly worse than those obtained using equations (22) and (23), therefore directing the successive investigations towards the benefits of using only *Fr* and the ratio $Y/Y_{cr}$.

Concerning the four different flow resistance equations, the comparison of the observed and simulated flow velocity values shown in Figure 8 and the statistics of Table 8 points out that the best performances are by the Limerinos, Iwagaki-Chow, and Hey equations. The Rickenmann and Recking equation has shown the lowest statistics overall, accentuating on average the tendency to overestimate the flow velocity values. The corresponding percentage error distributions allow identifying that the best performance is observed to be by the Limerinos equation, which in the 75% of the cases provided an estimate of the *U* values included between + and −20%. For the Iwagaki-Chow and Hey equations, these percentages were decreased to the 71% and 62%, respectively, and the Rickenmann and Recking equation provided the lowest percentage, equal to the 59% (supporting information Figure S5).

### 5.2. Validation of the New Resistance Equations

The benefits of the combined action of *Fr* and the ratio $Y/Y_{cr}$ become more evident in the case of river reaches characterized by very high bed load transport rate and very steep slope. If the new equations of Table 8 are directly validated using the measurements represented by the grey points of Figure 5, again the Limerinos equation allows obtaining the best performance (Table 8), even though it is appropriate to point out that the four equations are not able to entirely explain the increase in flow resistance produced by very high bed load transport rates, which results in higher estimation of the flow velocity values (Figure 9). However, the fact remains that in all the cases the resulting performances were considerably higher than those shown in Figure 8 and Table 6. In terms of percentage errors, the Limerinos equation provided the best performance with the 51% of the flow velocity estimates included between + and −20%, which increases up to 71% by considering the flow velocity estimates included between + and −30%. For the other equations, the percentage errors were concentrated for 80% within the class "−50% ÷ −30%" (supporting information Figure S6).

**Table 8**
*Coefficients of the Proposed Equations and Corresponding Statistics Obtained: For the Calibration Phase on the Enveloped Black Points Data Set in Figure 5 and for the Validation Phase on the Grey Points Data Set of the Same Figure*

| | | | | | Calibration | | | | Validation | | | |
|---|---|---|---|---|---|---|---|---|---|---|---|---|
| Equation | $b_1$ | $b_2$ | $b_3$ | $b_5$ | $R^2$ | RMSE | SI | IA | $R^2$ | RMSE | SI | IA |
| Limerinos | 0.041 | 0.30 | −0.47 | −0.05 | 0.82 | 0.15 | **17.07** | 0.95 | 0.63 | **0.16** | **24.10** | **0.88** |
| Hey | 15.00 | −0.23 | 0.36 | −12.00 | 0.90 | 0.15 | 18.02 | 0.95 | **0.89** | 0.28 | 41.91 | 0.71 |
| Iwagaki-Chow | 15.65 | −0.20 | 0.30 | −10.00 | **0.90** | **0.14** | 17.37 | **0.96** | 0.88 | 0.28 | 42.30 | 0.71 |
| Rickenmann and Recking | 14.30 | −0.25 | 0.30 | −12.00 | 0.84 | 0.18 | 20.95 | 0.93 | 0.80 | 0.31 | 47.42 | 0.60 |

*Note*. The bold values represent the best statistical indices values.

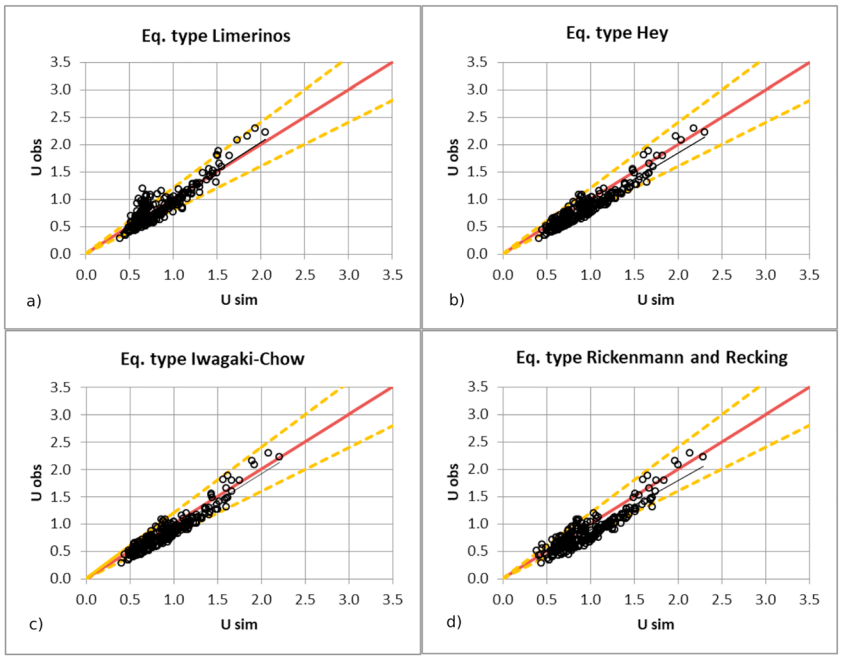


**Figure 8.** Comparison between observed and simulated flow velocity values for the whole enveloped black points data set in Figure 5, using modified equations of (a) Limerinos, (b) Hey, (c) Iwagaki-Chow, and (d) Rickenmann and Recking. The dashed yellow lines represent the + and −20% differences with respect to the observed values (the red line represents the line of perfect agreement).

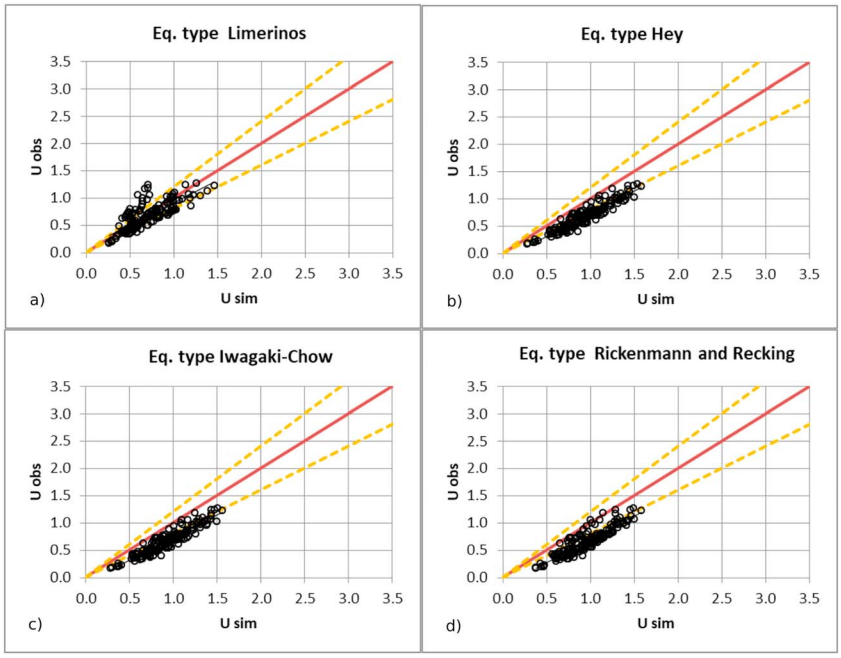


**Figure 9.** Comparison between observed and simulated flow velocity values for the grey points data set in Figure 5, using modified equations of (a) Limerinos, (b) Hey, (c) Iwagaki-Chow, and (d) Rickenmann and Recking. The dashed yellow lines represent the + and −20% differences with respect to the observed values (the red line represents the line of perfect agreement).

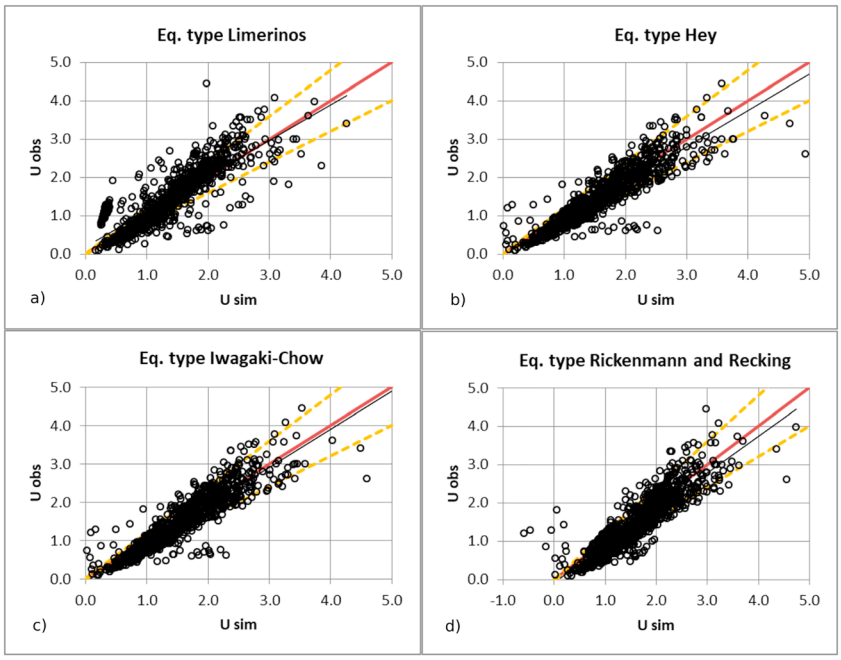


**Figure 10.** Comparison between observed and simulated flow velocity values for the literature-based data set in Figure 7 characterized by small- and intermediate-scale roughness ($R/d_{84} > 1.2$), using modified equations of (a) Limerinos, (b) Hey, (c) Iwagaki-Chow, and (d) Rickenmann and Recking. The dashed yellow lines represent the + and −20% differences with respect to the observed values (the red line represents the line of perfect agreement).

A second validation phase was carried out considering the literature-based data set described in Table 5. Of this data set, initially, only the measurements characterized by relative submergence values $R/d_{84} > 1.2$ were considered (1,049 cross sections corresponding to the black rectangles of Figure 6). This because the new equations were obtained considering data characterized for 98.53% by small- and intermediate-scale roughness (Table 2) and, therefore, not completely suitable for representing large-scale roughness. For this analysis, Figure 10 shows the comparison between observed and simulated flow velocity values, while in Table 9 the statistics resulting from the use of the new equations are given. Also, in this case, more than satisfactory performances for all the equations considered were observed, with slightly better statistical indices for the Iwagaki-Chow and the Hey equations. In the case of the Rickenmann and Recking equation, the performance was degraded by the fact there are four predictions of negative flow velocity values and obtained for small flow depth and relative submergence just above the threshold of 1.2. For what concerns the percentage errors, the Iwagaki-Chow (63%), Limerinos (62%), and Hey (60%) equations provided a quite similar behavior with the flow velocity estimates included between + and −20%. Finally, for the Rickenmann and Recking equation, only 53% of the flow velocity estimates were included between + and −20% of error (supporting information Figure S7).

**Table 9**
*Statistics Obtained Using the Proposed Equations on the Literature-Based Data Set in Figure 7 Characterized by Small- and Intermediate-Scale Roughness*

| | Validation | | | |
|---|---|---|---|---|
| Equation | $R^2$ | RMSE | SI | IA |
| Limerinos | 0.69 | 0.42 | 28.45 | 0.90 |
| Hey | 0.82 | 0.34 | 23.12 | 0.94 |
| Iwagaki-Chow | **0.82** | **0.32** | **21.57** | **0.95** |
| Rickenmann and Recking | 0.78 | 0.38 | 25.86 | 0.92 |

*Note*. The bold values represent the best statistical indices values.

### 5.3. Proposal of New Resistance Equations for Large-Scale Roughness

In the previous section, we specified that the new equations of Table 8 were obtained mainly considering small- and intermediate-scale roughness, and this makes them unsuitable in the case of large-scale roughness. This has been verified validating the same equations on the whole literature-based data set and, specifically, observing for each of them a great amount of predicted negative flow velocities.

This circumstance has led us to recalibrate the equations (22) and (23) using the 708 measurements of Table 5 characterized by relative

**Table 10**
*Coefficients of the Proposed Equations and Corresponding Statistics Obtained for the New Calibration Phase on the Literature-Based Data Set in Figure 7 Characterized by Large-Scale Roughness ($R/d_{84} < 1.2$)*

| | | | | | Calibration | | | | |
|---|---|---|---|---|---|---|---|---|---|
| Equation | $b_1$ | $b_2$ | $b_3$ | $b_5$ | $R^2$ | RMSE | SI | IA | *n.v.*[a] |
| Limerinos | 0.026 | 0.85 | −1.47 | −0.05 | **0.88** | **0.12** | **28.15** | **0.97** | 18 |
| Hey | 2.81 | −0.47 | 0.36 | −3.00 | 0.67 | 0.19 | 44.38 | 0.90 | 42 |
| Iwagaki-Chow | 2.96 | −0.45 | 0.35 | 0.00 | 0.68 | 0.19 | 43.99 | 0.90 | 42 |
| Rickenmann and Recking | 3.50 | −0.40 | 0.33 | −2.50 | 0.80 | 0.20 | 44.68 | 0.90 | 2 |

*Note*. The bold values represent the best statistical indices values.
[a]Predicted negative flow velocity values.

submergence values lower than 1.2 (black rhombus of Figure 6). It is useful to point out that also in this case we investigated the benefits produced by the Reynolds number, according to equations (20) and (21), observing no improvement in the performance of the flow resistance equations. Table 10 shows the coefficients of the new equations valid for large-scale roughness, together with the corresponding statistical indices values and the number of predicted negative flow velocities.

The performances obtained were more than satisfactory for all the considered equations, much higher than those provided by recent studies in the field of large-scale roughness. As an example, we report the performance obtained on the 708 measurements of Table 5 using the modified Manning-Strickler formula for large-scale roughness suggested by Cheng (2017) which, specifically provided significantly lower statistical indices ($R^2 = 0.40$). Among the new equations just determined, the best performance is observed to be by the Limerinos equation, even though the same equation shows 18 negative flow velocity values. Concerning the negative flow velocities, the Rickenmann and Recking equation behaves much better than the previous equation, because while showing statistical parameters lower, it allows a reduction in the negative flow velocity estimates to only two cross sections (Figure 11). In terms of percentage errors, the

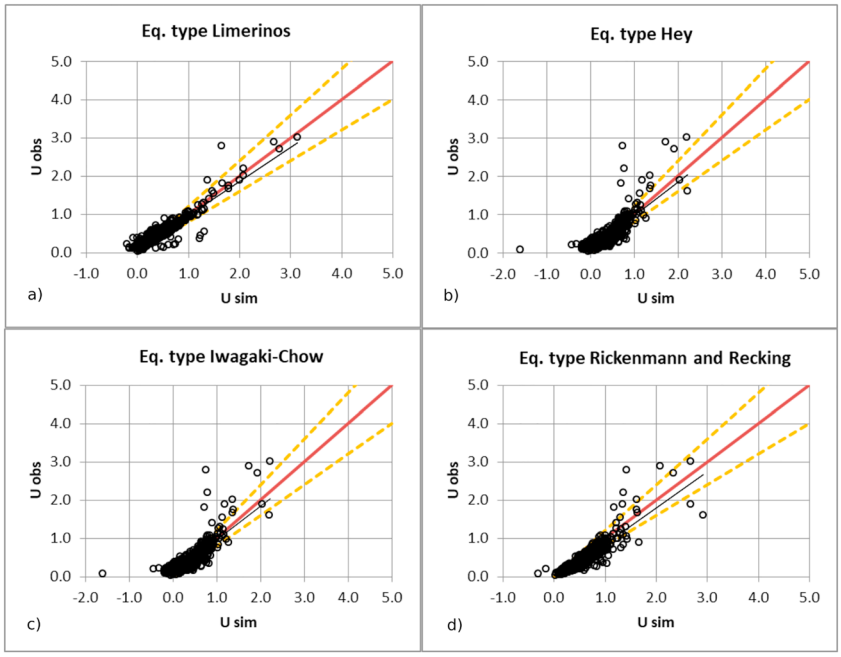


**Figure 11.** Comparison between observed and simulated flow velocity values for the literature-based data set in Figure 7 characterized by large-scale roughness ($R/d_{84} < 1.2$), using modified equations of (a) Limerinos, (b) Hey, (c) Iwagaki-Chow, and (d) Rickenmann and Recking. The dashed yellow lines represent the + and −20% differences with respect to the observed values (the red line represents the line of perfect agreement).

Limerinos equation continued to provide the best performance with the 75% of the flow velocity estimates included between + and −20%. The Iwagaki-Chow (48%) and the Hey (49%) equations provided a quite similar behavior with the flow velocity estimates included between + and −20%. For the Rickenmann and Recking equation, only 27% of the flow velocity estimates were included between + and −20% of error (supporting information Figure S8).

As a final step, we validated these new equations on the Calabrian data set characterized by relative submergence values lesser than 1.2. The six available observations certainly do not determine an unequivocal result but confirm the best performance to be by the Limerinos equation with respect to the others, and also observing very low relative submergence values, no negative flow velocities were obtained (supporting information Figure S9).

## 6. Discussion

The results shown so far have highlighted the benefits produced by the combined action of the Froude number and the ratio $Y/Y_{cr}$ on the flow resistance estimation. In general, when water surface distortions caused by boulder drag, wake vortices, local hydraulic jumps, and jetting of flow occur, then an additional energy loss has to be taken into account. This added resistance can be explained through the Froude number (Rouse et al., 1963), and it is due to the hydrostatic pressure imbalance generated by the superelevation and subelevation of the free surface around individual roughness elements (Lawrence, 2000). According to Bathurst (1982), when $Fr$ increases the degree of submergence usually increases too and the number of elements affecting the free surface and the drag of elements decrease. This means that the friction factor is inversely related to the Froude number (Bathurst et al., 1981). Different flow resistance equations confirmed Bathurst's hypothesis (Afzalimehr & Anctil, 1998; Colosimo et al., 1988; Di Stefano et al., 2018; Wang & Dawdy, 2014). Also, in the case of the Manning roughness coefficient, it can be observed that $n$ is inversely related to the Froude number (Camacho & Yen, 1991; Dìaz, 2005; Ugarte Soto & Madrid-Aris 1994; Zhang et al. 2010). The Calabrian data set herein utilized (Figure 5) confirmed this behavior, with coefficient $b_3$ values equal to −0.47 for the Limerinos equation, to 0.36 for the Hey equation, to 0.30 for the Iwagaki-Chow equation, and to 0.30 for the Rickenmann and Recking equation. Passing from small-/intermediate-scale roughness to large-scale roughness, higher flow resistance values should be explained, in the case of the Limerinos equation, by a lower $b_3$ value and, for the other equations, by higher $b_3$ values. This happens more clearly with the Limerinos equation ($b_3 = -1.47$) which, in particular, provides the highest performance. Furthermore, many researchers have widely demonstrated that the bed load increases the flow resistance (Baiamonte & Ferro, 1997; Bergeron & Carbonneau, 1999; Campbell et al., 2005; Carbonneau & Bergeron, 2000; Ferro, 2018b; Gao & Abrahams, 2004; Recking et al. 2008; Smart & Jaeggi, 1983; Song et al., 1995), because it extracts momentum from the flow, which causes a reduction in flow velocity and an increase in the apparent roughness length in proportions that are related to the thickness of the moving sediment layer. Specifically, Song et al. (1995) explained the phenomenon taking into account that particle motion determines a collision with particles lying on the bed or with each other. Then, an increase in the transport rate is associated with an increase in the frequency of particle collision resulting in an increase in energy loss. According to Gao and Abrahams (2004), during bed load transport, flow momentum is transferred from the fluid to bed through a two-step process, termed *bedload transport resistance*: (1) The momentum is transferred to the bed grains which are lifted from the bed and are accelerated by flow; (2) the momentum is lost when the particles impact with the bed, collide with other grains either resting on the bed or moving in the flow. The research carried out by Ferro (2018b) is also interesting about the dimensional analysis and the self-similarity theory used to theoretically establish the flow-resistance law under bed-load transport conditions. The incomplete self-similarity hypothesis is applied to theoretically deduce a flow velocity profile which takes into account the bed load transport condition by the Shields parameter.

Therefore, according to these considerations, we assume that this energy loss can be adequately explained by the increase in the shear stress and, hence, by the increase in the Yalin parameter $Y$. The use of the ratio $Y/Y_{cr}$ introduces in the equations (22) and (23) a dimensionless factor that increases or decreases the flow resistance according to the increase or reduction of the bed load transport rate, without considering energy dissipation processes that can occur over dunes, antidunes, ripples, and standing waves. The performances obtained reproducing the measurements related to domain 2 (moderate bed load transport rate) of

Figure 4 (Figure 8) allow a positive evaluation of the contribution provided by the ratio $Y/Y_{cr}$. This contribution becomes even bigger when measurements related to domain 3 (high bed load transport rate) of Figure 4 are reproduced (Figure 9).

Concerning the choice of using a constant $Y_{cr}$ value (in our case 0.029—Ackers & White, 1973), there are many contributions that showed the critical shear stress depending on the average channel gradient (Lamb et al., 2008; Mueller et al., 2005; Recking, 2009; Recking et al., 2008). In relation to our data set, we have also hypothesized a $Y_{cr}$ value varying with the slope, but the results obtained were not such as to justify further parameters in the new equations. More specifically, it has been observed that for river reaches characterized by increasing $D_{gr}$ values the influence of the slope in the estimation of $Y_{cr}$ became smaller and smaller.

Moreover, Recking et al. (2008) point out that the wakes that are shed as sediment grains are accelerated by the flow produce a roughness layer that develops well beyond the top of the saltation layer, affecting the mean velocity profile. Campbell et al. (2005) underlined the way in which it is characterized by a zone of intense turbulent kinetic energy production, whose thickness would increase really with the sediment size. If the mean flow velocity profile is affected by momentum extraction and the wake shed by accelerating grains as the bed load transport rate is increased, Recking et al. (2008) suggested increasing the equivalent bed roughness $k_s$ ($k_s = \alpha_{BR} d$) as relative depth $R/d$ increases. This hypothesis is equal to considering the additional term $\boldsymbol{f}(Y/Y_{cr}, Fr)$, because if it is applied according to equations (22) and (23) it determines a progressive downward shift of the Keulegan-based equations, which allows the overestimation of the flow velocities to be substantially reduced. This condition produces benefits not only when relative depth $R/d$ increases but also for low values of relative submergence. In this last case, it has been observed that for large-scale roughness the additional term $\boldsymbol{f}(Y/Y_{cr}, Fr)$ restricts the nonphysical predictions of the negative flow velocity values that the log-law approach shows when very small flow depths are considered.

Even though our approach is not derived from a rigorous physical analysis like that suggested by Flammer et al. (1970), nothing about it is incompatible with known physics. Furthermore, such as reported in Mueller et al. (2005), the process that drives bed load transport in gravel- and cobble-bed streams changes in several important ways as channel gradient increases, and for high slopes, there are also changes in flow structure (regime) that act independently of changes in sediment texture to alter transport thresholds (Sumer et al., 2003). This implies that it is not possible to discern the benefits that $Fr$ and $Y/Y_{cr}$ individually produce. Just from their combined action obviously better flow resistance estimations are obtained.

If, for example, the Limerinos equation is considered to estimate the average flow velocity using the whole enveloped black points data set of Figure 5, and the added resistance is expressed once as a function of the Froude number only, $\boldsymbol{f}(Fr)$, and then as a function of the ratio $Y/Y_{cr}$ only, $\boldsymbol{f}(Y/Y_{cr})$, it is possible to observe lower performance (supporting information Figure S10) compared to those obtained through the additional equation (22). However, this apparently obvious fact allows us to demonstrate the absence of spurious correlations because a different behavior of the $\boldsymbol{f}(Y/Y_{cr})$ with respect to the $\boldsymbol{f}(Fr)$ is observed. Specifically, this analysis points out in the field of micro- and intermediate-scale roughness the importance of the $\boldsymbol{f}(Y/Y_{cr})$ in the flow resistance estimation compared to the use of the $\boldsymbol{f}(Fr)$, such as shown by the exponent of each function (0.192 for $Y/Y_{cr}$ and −0.048 for $Fr$). The former not only provides better statistics but, such as shown in supporting information Figure S10, it compensates for a systematic overestimation of the flow velocities that instead are clearly observable in the latter. If the same analysis is carried out on the literature-based data set of Figure 7 characterized by large-scale roughness (supporting information Figure S11), we observe differently the more incisive action of the $\boldsymbol{f}(Fr)$ (better statistics for $Fr$ and exponents of the functions equal to 0.424 for $Y/Y_{cr}$ and −1.094 for $Fr$), but also in this case, the effect of the $\boldsymbol{f}(Y/Y_{cr})$ compensates for the overestimation of flow velocities observed with the $\boldsymbol{f}(Fr)$, which in the case of the large-scale roughness are further increased (supporting information Figure S11).

Therefore, all the new flow resistance equations with the additional term $\boldsymbol{f}(Y/Y_{cr}, Fr)$ provided, both in the calibration and in the validation phase, very high performances reproducing at the best measurements characterized by intermediate- and small-scale roughness, as well as flow velocities in river reaches characterized by very high values of bed load transport rate and steep channels. Among these equations, the Limerinos equation was found the best overall:

$$n = \frac{R^{1/6}\,0.1129}{1.16 + 2.0\log\left(\frac{R}{d_{84}}\right)} + \left(0.041\left(\frac{Y}{Y_{cr}}\right)^{0.30} Fr^{-0.47}\right) - 0.05 \quad (24)$$

with the following reliability limits: $1.20 < R/d_{84} < 520.65$; $0.04 < Fr < 2.17$; $0.02 < Y/Y_{cr} < 29.06$.

Also, in the case of large-scale roughness measurements, the recalibrated new equations provided performances more than satisfactory, and in particular, the Limerinos equation shown again the best results:

$$n = \frac{R^{1/6}\,0.1129}{1.16 + 2.0\log\left(\frac{R}{d_{84}}\right)} + \left(0.026\left(\frac{Y}{Y_{cr}}\right)^{0.85} Fr^{-1.47}\right) - 0.05 \quad (25)$$

with the following reliability limits: $0.14 < R/d_{84} < 1.20$; $0.03 < Fr < 1.15$; $0.02 < Y/Y_{cr} < 6.00$.

## 7. Conclusion

Through a new data set of field measurements carried out on 136 reaches of 78 gravel-bed rivers in southern Italy, covering a wide range of geometric, granulometric, hydraulic, and sediment parameters, different conventional flow resistance equations (Bathurst, 1985; Ferguson, 2007; Hey, 1979; Iwagaki-Chow, 1959; Jarrett, 1984; Keulegan, 1938; Limerinos, 1970; Rickenmann & Recking, 2011; Smart & Jaeggi, 1983; Strickler, 1923) were analyzed in their original form to test the suitability to predict mean flow velocity in gravel-bed rivers. The results obtained have shown that some of these equations have to be used with extreme caution (Strickler, Keulegan, and Iwagaki-Chow), especially in the intermediate- and the large-scale roughness domains where marked overestimation of flow velocities occurred. The other equations showed almost similar performances with slight improvements in the case of the VPE-based equations (Ferguson, 2007; Rickenmann & Recking, 2011). These small differences, however, tend to disappear in the field of small-scale roughness.

Furthermore, the same data set allowed pointing out the inadequacy of all the considered equations when applied in river reaches characterized by very high values of bed load transport rate and steep channels. In this context, only the Jarrett equation provided acceptable performances for all the considered relative submergence classes.

Then, we investigated the benefits produced by the Froude number and the ratio $Y/Y_{cr}$ on four different flow resistance equations (Hey, 1979; Iwagaki-Chow, 1959; Limerinos, 1970; Rickenmann & Recking, 2011) adding to the original structure a term $\boldsymbol{f}(Y/Y_{cr}, Fr)$. All the new flow resistance equations have provided, both in the calibration phase and in the validation, very high performances reproducing at the best measurements characterized by intermediate- and small-scale roughness, as well as flow velocities in river reaches characterized by very high values of bed load transport rate and steep channels. Among these equations, the Limerinos equation was found the best overall.

Since in the new Calabrian data set there were not a significant number of large-scale roughness measurements, in order to extend the application field of the new equations into the large-scale roughness domain, the same equations were recalibrated using 708 literature measurements characterized by relative submergence values $R/d_{84} < 1.2$. Also, in this case, the performances obtained were more than satisfactory and, in particular, the Limerinos equation shown again the best results.

Based on what has been shown, this study led to the following conclusions:

1. The conventional flow resistance equations herein considered, when evaluated in their original form were found to be reliable only for small-scale roughness and absence of bed load transport, instead the same equations have to be used with extreme caution, both in the intermediate- and the large-scale roughness domains and, especially, when river reaches characterized by very high values of bed load transport are analyzed;
2. Compared with many studies conducted in the past in which was shown the benefit of only the Froude number in the flow resistance estimation, the paper shows the improvements obtained by introducing the ratio $Y/Y_{cr}$ in the flow velocity estimates; also showing how the combined action of the Froude

number and the ratio $Y/Y_{cr}$ allows to take into account those losses due to water surface distortion caused by boulder drag, wake vortices, local hydraulic jumps, and jetting of flow, as well as the reduction in flow velocity caused by the bed load, which differently are not evaluated within the conventional flow resistance equations.

3. The analyses carried out have shown that the conventional equations, even though with differences more or less marked among them, are not able to go beyond a certain limit of performance. The additional term $\boldsymbol{f}(Y/Y_{cr}, Fr)$ not only allowed to improve a lot the flow velocity estimates but also directed toward a reconsideration of equations, such as that of Limerinos in the small-, intermediate-, and large-scale roughness domains or also that of Iwagaki-Chow in the intermediate- and small-scale roughness domains, considered outdated with respect to other more recent equations suggested in literature.

**Acknowledgments**
The authors acknowledge valuable comments from D. Scott Mackay (Editor), Vito Ferro, and two anonymous reviewers, which led to significant improvement of the paper. All the results/data have been included in the paper and supporting information.

## References

Ackers, P., & White, W. R. (1973). Sediment transport: New approach and analysis. *Journal of Hydraulics Division, ASCE*, *99*, 2041–2060.

Adenlof, K. A., & Wohl, E. E. (1994). Controls on bed load movement in a subalpine Stream of the Colorado Rocky Mountains, U.S.A. *Journal of Arctic and Alpine Research*, *26*(1), 77–85. https://doi.org/10.2307/1551881

Afzalimehr, H., & Anctil, F. (1998). Estimation of gravel-bed river flow resistance. *Journal of Hydraulic Engineering*, *124*(10), 1054–1058. https://doi.org/10.1061/(ASCE)0733-9429(1998)124:10(1054)

Andrews, E. D. (1994). Marginal bed load transport in a gravel bed stream, Sagehen Creek, California. *Water Resources Research*, *30*(7), 2241–2250. https://doi.org/10.1029/94WR00553

Baiamonte, G., & Ferro, V. (1997). The influence of roughness geometry and Shields parameter on flow resistance in gravel-bed channels. *Earth Surface Processes and Landforms*, *22*, 759–772. https://doi.org/10.1002/(SICI)1096-9837(199708)22:8<759:AID-ESP779>3.0.CO;2-M

Bathurst, J. C. (1982). Flow resistance in boulder-bed streams. In R. D. Hey, J. C. Bathurst, & C. R. Thorne (Eds.), *Gravel-Bed Rivers: Fluvial Processes, Engineering and Management* (pp. 443–465). Chichester: John Wiley.

Bathurst, J. C. (1985). Flow resistance estimation in mountain rivers. *Journal of Hydraulic Engineering*, *111*(4), 625–643. https://doi.org/10.1061/(ASCE)0733-9429(1985)111:4(625)

Bathurst, J. C. (2002). At-a-site variation and minimum flow resistance for mountain rivers. *Journal of Hydrology*, *269*(1-2), 11–26. https://doi.org/10.1016/S0022-1694(02)00191-9

Bathurst, J. C., Li, R. M., & Simons, D. B. (1981). Resistance equation for large-scale roughness. *Journal of Hydraulics Division, ASCE*, *107*, 1593–1613.

Bergeron, N. E., & Carbonneau, P. (1999). The effect of sediment concentration on bedload roughness. *Hydrological Processes*, *13*, 2583–2589. https://doi.org/10.1002/(SICI)10991085(199911)13:16<2583:AID-HYP939>3.0.CO;2-S

Bray, D. I. (1979). Estimating average velocity in gravel-bed rivers. *Journal of Hydraulics Division, ASCE*, *105*, 1103–1122.

Camacho, R., & Yen, B. C. (1991). Nonlinear resistance relationships for alluvial channels, in *Channel flow resistance: Centennial of Manning's* formula by Ben Chie Yen, editor, *Water Resources Publication*, 114, 186–194, Littleton, Colorado, USA.

Campbell, L., McEwan, I., Nikora, V. I., Pokrajac, D., Gallagher, M., & Manes, C. (2005). Bed-load effects on hydrodynamics of rough-bed open-channel flows. *Journal of Hydraulic Engineering*, *131*(7), 576–585. https://doi.org/10.1061/(ASCE)0733-9429(2005)131:7(576

Carbonneau, P., & Bergeron, N. E. (2000). The effect of bedload transport on mean and turbulent flow properties. *Geomorphology*, *35*(3-4), 267–278. https://doi.org/10.1016/S0169-555X(00)00046-5

Charlton, F. G., Brown, P. M., & Benson, R. W. (1978). The hydraulic geometry of some gravel bed rivers in Britain, Report IT 180, Hydraulics Research Station Wallingford, England.

Cheng, N. S. (2017). Simple modification of Manning-Strickler formula for large-scale roughness. *Journal of Hydraulic Engineering*, *143*, 9. https://doi.org/10.1061/(ASCE)HY.1943-7900.0001345

Cheng, N. S., Liu, X., Chen, X., & Qiao, C. (2016). Deviation of permeable coarse-grained boundary resistance from Nikuradse's observations. *Water Resources Research*, *52*, 1194–1207. https://doi.org/10.1002/2015WR017666

Chow, V. T. (1959). *Open-channel hydraulics*. New York: McGraw-Hill.

Church, M., & Rood, K. (1983). Catalogue of alluvial channel regime data, 99–100 pp., Department of Geography, University of British Columbia. Retrieved from http://www.nced.umn.edu/

Colosimo, C., Copertino, V., & Veltri, M. (1988). Friction factor evaluation in gravel-bed rivers. *Journal of Hydraulic Engineering*, *114*(8), 861–876. https://doi.org/10.1061/(ASCE)0733-9429(1988)114:8(861)

Colosimo, C., Veltri, M., & Mendicino, G. (1991). Froude number in evaluation of resistance coefficient in natural rivers, in *Channel flow resistance: Centennial of Manning's* formula by Ben Chie Yen, editor, *Water Resources Publication*, 114, 309–317, Littleton, Colorado, USA.

Comiti, F., Mao, L., Wilcox, A., Wohl, E., & Lenzi, M. (2007). Field derived relationships for flow velocity and resistance in high-gradient streams. *Journal of Hydrology*, *340*(1-2), 48–62. https://doi.org/10.1016/j.jhydrol.2007.03.021

David, G. C. L., Wohl, E. E., Yochum, S. E., & Bledsoe, B. P. (2010). Controls on spatial variations in flow resistance along steep mountain streams. *Water Resources Research*, *46*, W03513. https://doi.org/10.1029/2009WR008134

Di Stefano, C., Ferro, V., Palmeri, V., & Pampalone, V. (2018). Testing slope effect on flow resistance equation for mobile bed rills. *Hydrological Processes*, *32*(5), 664–671. https://doi.org/10.1002/hyp.11448

Diaz, R. G. (2005). Analysis of Manning coefficient for small-depth flows on vegetated beds. *Hydrological Processes*, *19*(16), 3221–3233. https://doi.org/10.1002/hyp.5820

Ferguson, R. (2007). Flow resistance equations for gravel and boulder bed streams. *Water Resources Research*, *43*, W05427. https://doi.org/10.1029/2006WR005422

Ferguson, R. (2010). Time to abandon the Manning equation? *Earth Surface Processes and Landforms*, *35*(15), 1873–1876. https://doi.org/10.1002/esp.2091

Ferro, V. (1999). Friction factor for gravel bed channel with high boulder concentration. *Journal of Hydraulic Engineering*, *125*(7), 771–778. https://doi.org/10.1061/(ASCE)0733-9429(1999)125:7(771)
Ferro, V. (2003). Flow resistance in gravel-bed channels with large-scale roughness. *Earth Surface Processes and Landforms*, *28*(12), 1325–1339. https://doi.org/10.1002/esp.589
Ferro, V. (2017). New flow-resistance law for steep mountain streams based on velocity profile. *Journal of Irrigation and Drainage Engineering*, *143*(8), 04017024. https://doi.org/10.1061/(ASCE)IR.1943-4774.0001208
Ferro, V. (2018a). Assessing flow resistance in gravel bed channels by dimensional analysis and self-similarity. *Catena*, *169*, 119–127. https://doi.org/10.1016/j.catena.2018.05.034
Ferro, V. (2018b). Flow resistance law under equilibrium bed-load transport condition. *Flow Measurement and Instrumentation*, *64*, 1–8. https://doi.org/10.1016/j.flowmeasinst.2018.10.008
Ferro, V., & Porto, P. (2018). Applying hypothesis of self-similarity for flow-resistance law in Calabrian gravel-bed rivers. *Journal of Hydraulic Engineering*, *144*, 2. https://doi.org/10.1061/(ASCE)HY.1943-7900.0001385
Flammer, G. H., Tullis, J. P., & Mason, E. S. (1970). Free surface velocity gradient flow past hemisphere. *Journal of Hydraulic Engineering*, *96*(7), 1485–1502.
Gao, P., & Abrahams, A. D. (2004). Bedload transport resistance in rough open-channel flows. *Earth Surface Processes and Landforms*, *29*(4), 423–435. https://doi.org/10.1002/esp.1038
Graf, W. H. (1984). Flow resistance for steep, mobile channels, In Proceedings of Workshop on 'Idraulica del territorio montano', Bressanone, Italy.
Graf, W. H., Cao, H. H., & Suszka, L. (1983). Hydraulics of step mobile-bed channels, Proceedings of 20th Congress of the International Association for Hydraulic Research, Moscow, URSS.
Griffiths, G. A. (1981). Flow resistance in coarse gravel bed rivers. *Journal of Hydraulics Division, ASCE*, *107*(HY7), 899–918.
Hey, R. D. (1979). Flow resistance in gravel-bed rivers. *Journal of Hydraulics Division, ASCE*, *105*, 365–379.
Hey, R. D., & Thorne, C. R. (1986). Stable channels with mobile gravel beds. *Journal of Hydraulic Engineering*, *112*(8), 671–689. https://doi.org/10.1061/(ASCE)0733-9429(1986)112:8(671)
Iwagaki, Y. (1954). On the law of resistance to turbulent flow in open rough channels, Proceedings of the 4th Japan National Congress for Applied Mechanics, 229-233.
Jarrett, R. D. (1984). Hydraulics of high-gradient streams. *Journal of Hydraulic Engineering*, *110*(11), 1519–1539. https://doi.org/10.1061/(ASCE)0733-9429(1984)110:11(1519)
Jones, M. L., & Seitz, H. R. (1979). Suspended- and bedload-sediment transport in the snake and clear water rivers in the vicinity of Lewiston, Idaho, fifth basic-data report, Prepared in cooperation with the U.S. Army Corps of Engineers, Walla Walla District.
Keulegan, G. H. (1938). Laws of turbulent flow in open channels. *Journal of Research of the National Bureau of Standarss. U.S.*, *21*(6), 707–741. https://doi.org/10.6028/jres.021.039
Lamb, M. P., Dietrich, W. E., & Venditti, J. G. (2008). Is the critical Shields stress for incipient sediment motion dependent on channel-bed slope? *Journal of Geophysical Research*, *113*, F02008. https://doi.org/10.1029/2007JF000831
Lawrence, D. S. L. (1997). Macroscale surface roughness and frictional resistance in overland flow. *Earth Surface Processes and Landforms*, *22*(4), 365–382. https://doi.org/10.1002/(SICI)1096-9837(199704)22:4<365::AID-ESP693>3.0.CO;2-6
Lawrence, D. S. L. (2000). Hydraulic resistance in overland flow during partial and marginal surface inundation: Experimental observations and modeling. *Water Resources Research*, *36*(8), 2381–2393. https://doi.org/10.1029/2000WR900095
Leopold, L. B., & Emmett, W. W. (1976). Bedload measurements, East Fork River, Wyoming. *Proceedings of the National Academy of Sciences of the United States of America*, *73*(4), 1000–1004. https://doi.org/10.1073/pnas.73.4.1000
Limerinos, J. T. (1970). Determination of the Manning coefficient from measured bed roughness in natural channels, United States Geological Survey Water Supply Paper, 1898-B, 47 pp.
MacKenzie, L. G., Brett, C. E., & Church, M. (2018). Breaking from the average: Why large grains matter in gravel-bed streams. *Earth Surface Processes and Landforms*, *43*(15), 3190–3196. https://doi.org/10.1002/esp.4465
Mueller, E. R., Pitlick, J., & Nelson, J. M. (2005). Variation in the reference Shields stress for bed load transport in gravel-bed streams and rivers. *Water Resources Research*, *41*, W04006. https://doi.org/10.1029/2004WR003692
Nakato, T., Locher, F. A., Glover, J. R., & Kennedy, J. F. (1977). Iowa sediment concentration measuring system. *Journal of Hydraulics Division, ASCE*, 2060–2071. https://doi.org/10.1061/9780872620834.120
Namaee, M. R., Sui, J., & Whitcombe, T. (2017). A revisit of different models for flow resistance in gravel-bed rivers and hydraulic flumes. *International Journal of River Basin Management*, *15*(3), 277–286. https://doi.org/10.1080/15715124.2017.1287710
Nikora, V., Goring, D., McEwan, I., & Griffiths, G. (2001). Spatially averaged open-channel flow over rough bed. *Journal of Hydraulic Engineering*, *127*(2), 123–133. https://doi.org/10.1061/(ASCE)0733-9429(2001)127:2(123)
Nitsche, M., Rickenmann, D., Kirchner, J. W., Turowski, J. M., & Badoux, A. (2012). Macroroughness and variations in reach-averaged flow resistance in steep mountain streams. *Water Resources Research*, *48*, W12518. https://doi.org/10.1029/2012WR012091
Orlandini, S., Boaretti, C., Guidi, V., & Sfondrini, G. (2006). Field determination of the spatial variation of resistance to flow along a steep Alpine stream. *Hydrological Processes*, *20*(18), 3897–3913. https://doi.org/10.1002/hyp.6163
Pemberton, E. (1964). Sediment investigations—Middle Rio Grande. *Journal of Hydraulics Division, ASCE*, *90*(2), 163–185.
Powell, D. M. (2014). Flow resistance in gravel-bed rivers: Progress in research. *Earth-Science Reviews*, *136*, 301–338. https://doi.org/10.1016/j.earscirev.2014.06.001
Recking, A. (2009). Theoretical development on the effects of changing flow hydraulics on incipient bed load motion. *Water Resources Research*, *45*, W04401. https://doi.org/10.1029/2008WR006826
Recking, A., Frey, P., Paquier, A., Belleudy, P., & Champagne, J. Y. (2008). Feedback between bed load and flow resistance in gravel and cobble bed rivers. *Water Resources Research*, *44*, W05412. https://doi.org/10.1029/2007WR006219
Reid, D. E., & Hickin, E. J. (2008). Flow resistance in steep mountain streams. *Earth Surface Processes and Landforms*, *33*(14), 2211–2240. https://doi.org/10.1002/esp.1682
Rickenmann, D., & Recking, A. (2011). Evaluation of flow resistance in gravel-bed rivers through a large field data set. *Water Resources Research*, *47*, W07538. https://doi.org/10.1029/2010WR009793
Rosso, M., Schiara, M., & Berlamont, J. (1990). Flow stability and friction factor in rough channels. *Journal of Hydraulic Engineering*, *116*(9), 1109–1118. https://doi.org/10.1061/(ASCE)0733-9429(1990)116:9(1109)
Rouse, H., Koloseus, H. J., & Davidian, J. (1963). The role of the Froude number in open channel resistance. *Journal of Hydraulic Research*, *1*, 14–19.

Sabato, L., & Tropeano, M. (2004). Fiumara: A kind of high hazard river. *Physics and Chemistry of the Earth*, *29*(10), 707–715.
Shields, A. (1936). Anwendung der Aehnlichkeitsmechanik und der Turbulenzforschung auf die Geschiebebewegung, Mitteilungen der Preussichen Veruchsanstalt fur Wasserbau und Schiffbau, Heft 26, Germany.
Simons, D., & Albertson, M. (1960). Uniform water conveyance channels in alluvial material. *Journal of Hydraulics Division, ASCE*, *86*(5), 33–71.
Smart, G. M., & Jaeggi, M. N. R. (1983). Sediment transport on steep slopes. In *Mitteilungen der Versuchsanstalt f˙ur Wasserbau, Hydrologie und Glaziologie* (Vol. 64, pp. 89–191). Zürich, Zurich, Switzerland: Eidg. Tech. Hochsch.
Song, T., Graf, W. H., & Lemmin, U. (1995). Uniform flow in open channels with movable gravel bed. *Journal of Hydraulic Research*, *32*, 861–875.
Strickler, A. (1923). Beiträge zur Frage der Geschwindigkeits formel und der Rauhigkeitszahlen für Ströme, Kanäle und geschlossene Leitungen. *Mitt. 16*, Eidg. Amt für Wasserwirtsch.. Bern, Switzerland.
Sumer, B. M., Chua, L. H. C., Cheng, N. S., & Fredsoe, J. (2003). Influence of turbulence on bed load sediment transport. *Journal of Hydraulic Engineering*, *129*(8), 585–596. https://doi.org/10.1061/(ASCE)0733-9429(2003)129:8(585)
Thompson, S. M., & Campbell, P. L. (1979). Hydraulics of a large channel paved with boulders. *Journal of Hydraulic Research*, *17*(4), 341–354. https://doi.org/10.1080/00221687909499577
Thorne, C. L., & Zevenbergen, L. W. (1985). Estimating mean velocity in mountain rivers. *Journal of Hydraulic Engineering*, *111*(4), 612–624. https://doi.org/10.1061/(ASCE)0733-9429(1985)111:4(612
Ugarte Soto, A., & Madrid-Aris, M. (1994). Roughness coefficient in mountain river. In G. V. Cotroneo & R. Rumer (Eds.), *Hydraulic Engineering* (Vol. 1, pp. 652–656). New York: American Society of Civil Engineers.
Wang, W. C., & Dawdy, D. R. (2014). Flow resistance of gravel bed channels. *International Journal of Sediment Research*, *29*(1), 126–132. https://doi.org/10.1016/S1001-6279(14)60028-7
Wiberg, P. L., & Smith, J. D. (1991). Velocity distribution and bed roughness in high-gradient streams. *Water Resources Research*, *27*(5), 825–838. https://doi.org/10.1029/90WR02770
Wohl, E. (2000). *Mountain rivers, AGU Water Resource Monograph* (Vol. 14, p. 320). Washington, DC.
Wohl, E., & Wilcox, A. (2005). Channel geometry of mountain streams in New Zealand. *Journal of Hydrology*, *300*(1-4), 252–266. https://doi.org/10.1016/j.jhydrol.2004.06.006
Yalin, M. S. (1972). *Mechanics of sediment transport, 1st end* (Vol. 290). New York: Pergamon Press.
Yen, B. C. (1992). Hydraulic resistance in open channels, in *Channel flow resistance: Centennial of Manning's* formula by Ben Chie Yen, editor, *Water Resources Publication*, 114, 1–135, Littleton, Colorado, USA.
Yochum, S. E., Bledsoe, B. P., David, G. C. L., & Wohl, E. (2012). Velocity prediction in high-gradient channels. *Journal of Hydrology*, *424-425*, 84–98. https://doi.org/10.1016/j.jhydrol.2011.12.031
Zhang, G. H., Luo, R. T., Cao, Y., Rui, C. S., & Zhang, X. C. (2010). Impacts of sediment load on Manning coefficient in supercritical shallow flow on steep slopes. *Hydrological Processes*, *24*(26), 3909–3914. https://doi.org/10.1002/hyp.7892